HHS Public Access

Author manuscript

Nat Med. Author manuscript; available in PMC 2020 January 13.

Published in final edited form as:

Nat Med. 2017 January ; 23(1): 79–90. doi:10.1038/nm.4252.

Fasting selectively blocks development of acute lymphoblastic leukemia via leptin-receptor upregulation

Zhigang Lu[1,10], **Jingjing Xie**[1,2,10], **Guojin Wu**[1], **Jinhui Shen**[1], **Robert Collins**[3], **Weina Chen**[4], **Xunlei Kang**[1], **Min Luo**[5], **Yizhou Zou**[6], **Lily Jun-Shen Huang**[7], **James F Amatruda**[8], **Tamra Slone**[8], **Naomi Winick**[8], **Philipp E Scherer**[3,7,9], **Cheng Cheng Zhang**[1,2]

[1]Department of Physiology, University of Texas Southwestern Medical Center, Dallas, Texas, USA.

[2]BMU–UTSW Joint Taishan Immunology Group, Binzhou Medical University, Yantai, Shandong, China.

[3]Department of Internal Medicine, University of Texas Southwestern Medical Center, Dallas, Texas, USA.

[4]Department of Pathology, University of Texas Southwestern Medical Center, Dallas, Texas, USA.

[5]Harold C. Simmons Comprehensive Cancer Center, University of Texas Southwestern Medical Center, Dallas, Texas, USA.

[6]Department of Immunology, Central South University School of Xiangya Medicine, Changsha, Hunan, China.

[7]Department of Cell Biology, University of Texas Southwestern Medical Center, Dallas, Texas, USA.

[8]Department of Pediatrics, University of Texas Southwestern Medical Center, Dallas, Texas, USA.

[9]Touchstone Diabetes Center, University of Texas Southwestern Medical Center, Dallas, Texas, USA.

Abstract

New therapeutic approaches are needed to treat leukemia effectively. Dietary restriction regimens, including fasting, have been considered for the prevention and treatment of certain solid tumor types. However, whether and how dietary restriction affects hematopoietic malignancies is unknown. Here we report that fasting alone robustly inhibits the initiation and reverses the leukemic progression of both B cell and T cell acute lymphoblastic leukemia (B-ALL and T-ALL,

Correspondence should be addressed to Z.L. (zhigang.lu@utsouthwestern.edu) or C.C.Z (Alec.Zhang@UTSouthwestern.edu).

AUTHOR CONTRIBUTIONS

C.C.Z. and Z.L. designed experiments. C.C.Z. conceived the study. Z.L., J.X., G.W., J.S. and P.E.S. performed experiments and interpreted data. L.J.-S.H., X.K., Y.Z. and M.L. performed experiments. Z.L. and J.X. performed statistical analysis. R.C., W.C., J.F.A., T.S. and N.W. provided patient samples. The manuscript was written by C.C.Z. and Z.L. and contributed to by all authors.

[10]These authors contributed equally to this work.

Note: Any Supplementary Information and Source Data files are available in the online version of the paper.

COMPETING FINANCIAL INTERESTS

The authors declare no competing financial interests.

respectively), but not acute myeloid leukemia (AML), in mouse models of these tumors. Mechanistically, we found that attenuated leptin-receptor (LEPR) expression is essential for the development and maintenance of ALL, and that fasting inhibits ALL development by upregulation of LEPR and its downstream signaling through the protein PR/SET domain 1 (PRDM1). The expression of LEPR signaling-related genes correlated with the prognosis of pediatric patients with pre-B-ALL, and fasting effectively inhibited B-ALL growth in a human xenograft model. Our results indicate that the effects of fasting on tumor growth are cancer-type dependent, and they suggest new avenues for the development of treatment strategies for leukemia.

Dietary restriction, including fasting, delays aging and has pro-longevity effects in a wide range of organisms, and so has been considered for cancer prevention and the treatment of certain solid tumor types[1–6]. Fasting can promote hematopoietic stem cell–based regeneration and reverse immunosuppression[7–9], and has been reported to promote the anti-cancer effects of chemotherapy[5,10]. However, the responsiveness of hematopoietic malignancies to dietary restriction, including fasting, remains unknown.

AML is the most common form of adult acute leukemia, whereas ALL is the most common form of cancer in children; ALL also occurs in adults[11–13]. Although treatment of pediatric ALL is highly effective, a sizeable number of patients are nonresponders who succumb to this disease. The outcome of ALL in adults is substantially worse than for pediatric ALL, with a 5-year survival rate of approximately 40%[12]. Additionally, some types of ALL have a much poorer prognosis than others[12]. New therapeutic targets and approaches need to be identified to treat these leukemias more effectively. Here we investigated whether and how fasting regulates the development of B-ALL, T-ALL and AML.

RESULTS

Fasting selectively inhibits the development of ALL but not AML

To extend our previous work on the extrinsic and metabolic regulation of hematopoietic stem cells and cancer development[14–22], we studied the effects of fasting on leukemia development. Mice from several retrovirus transplantation acute leukemia models, including the N-Myc B-ALL model[23], the activated Notch1 T-ALL model[24] and the MLL-AF9 AML model[25,26], were placed on various dietary regimens. Strikingly, a regimen consisting of six cycles of 1 d of fasting, followed by 1 d of feeding, implemented 2 d after transplantation (Fig. 1a) completely inhibited B-ALL development. The fasted mice had 32.85 ± 5.16, 11.31 ± 5.42 and 0.48 ± 0.12% of leukemic GFP^+ cells in peripheral blood (PB) at 3, 5 and 7 weeks post-transplantation, respectively, as compared to 49.52 ± 5.75, 56.27 ± 9.36 and 67.68 ± 8.39% of GFP^+ cells of the control mice (Fig. 1b,c). Concordantly, the percentages of leukemic cells in the bone marrow (BM) and spleen (SP) and the numbers of white blood cells (WBCs) in PB were also dramatically lower in the fasted mice at 7 weeks post-transplantation (Fig. 1c,d).

Next, we measured the distribution of B lymphoblastic cells and myeloid cells in the GFP^+ compartment of the B-ALL mice. Control mice with B-ALL had 65–80% of $B220^+$ cells (pan B lineage marker) and 0.5–2% of $Mac\text{-}1^+$ cells (myeloid lineage marker) in GFP^+

fractions of PB, BM and SP (Fig. 1e,f), indicative of fully developed B-ALL. By contrast, there were only 19–28% of $B220^+$ cells and 5–12% of $Mac\text{-}1^+$ in GFP^+ fractions in fasted mice (Fig. 1e,f), consistent with loss of the B-ALL phenotype. There was also a higher percentage of differentiated $B220^+IgM^+$ cells in the GFP^+ compartment in fasted mice than in fed mice (Fig. 1g). These results suggest that fasting blocks B-ALL development by decreasing malignant B cell propagation and enhancing B cell differentiation.

In the fasted mice, the infiltration of B-ALL cells into the spleen and lymph nodes, as assessed by organ size, was also significantly decreased, such that the size of the spleen and lymph nodes in fasted mice was similar to that in normal mice (Fig. 1h). Fed, but not fasted, leukemic mice showed tissue destruction in the spleen and liver (Supplementary Fig. 1a). All fed mice with B-ALL died within 59 d after transplantation. In a striking contrast, 75% of their fasted counterparts survived for more than 120 d without any leukemia symptoms (Fig. 1i and Supplementary Fig. 1b–d). The small fraction of GFP^+ cells in these surviving mice behaved similarly to normal cells; secondary transplantation of these cells did not result in leukemic symptoms (Supplementary Fig. 2). We conclude that fasting dramatically inhibits B-ALL development.

In the Notch1 T-ALL model, six cycles of fasting resulted in a dramatic decrease of T-ALL development (Fig. 1j–m and Supplementary Fig. 3a). Fasting lowered the percentage of leukemic GFP^+ in PB, BM and SP over time (Fig. 1j), decreased WBC counts in the PB and maintained normal spleen and liver structure (Fig. 1k and Supplementary Fig. 3a). Fasted mice had a lower percentage of $CD3^+$ cells (T lineage marker) and a higher percentage of myeloid $Mac\text{-}1^+$ cells in the GFP^+ compartment, as compared to fed mice (Fig. 1l), and fasting significantly prolonged the survival of the T-ALL mice (Fig. 1m). Thus, this fasting regimen can block the development of T-ALL as well as B-ALL.

In striking contrast to the B-ALL and T-ALL models, fasted mice with MLL-AF9 AML did not show reductions in the percentages of leukemic YFP^+ cells, $Mac\text{-}1^+$ cells in the YFP^+ compartment or $Mac\text{-}1^+Kit^+$ AML progenitor cells, or in the colony-forming activity of YFP^+ BM cells (Fig. 1n–p and Supplementary Fig. 3b). Fasting significantly decreased the percentage of $B220^+$ B lineage cells in the YFP^+ compartment (Fig. 1o) and shortened the overall survival time of mice with AML (Fig. 1q). Similarly, fasting did not alter leukemia development in another AML mouse model, driven by the *AML1-Eto9a* oncogene[27] (Supplementary Fig. 4). Thus, fasting inhibits the development of ALL but not AML in mice.

Fasting inhibits ALL development at both early and late stages

We sought to understand whether fasting blocks ALL at tumor initiation or later during leukemia development. First, we tested the effects of varying the numbers of 1-d-fasting–1-d-feeding (1F) fasting cycles, started at day 2 after transplantation, on B-ALL development (Fig. 2a). Every increase of a fasting cycle for up to six cycles resulted in an improvement in leukemia inhibition; a four-cycle fasting regimen essentially eliminated B-ALL. With increased numbers of fasting cycles, we observed augmented decreases in the percentage of leukemic GFP^+ cells in PB, BM and SP, in the numbers of WBCs in PB and in leukemia burden rates, together with an increase in B-ALL mouse overall survival (Fig. 2b–e). We

also tested another fasting strategy with one to four cycles of 2-d-fasting–2-d-feeding cycles (2F) (Fig. 2a). We found that two cycles of 2F significantly reduced the development of B-ALL, and that three or four 2F cycles had equivalent effects to six cycles of 1F with regard to complete inhibition of B-ALL development, such that 80% of the mice survived longer than 120 d (Fig. 2f–i). Clearly, fasting at the tumor initiation stage effectively inhibits B-ALL development, and the level of inhibition correlates with the number of cycles of fasting.

Next, we tested the effect of fasting at a middle-to-late stage of B-ALL development. We began the fasting regimens—either two and four cycles of 1F fasting (hereafter 2–1F/4–1F) or two and three cycles of 2F fasting (hereafter 2–2F/3–2F) —when the percentage of leukemic GFP^+ cells in PB of primary recipients had reached ~60% (Fig. 2a). Whereas the percentage of GFP^+ cells in PB rose over time in control mice, this percentage decreased dramatically at 2 and 3 weeks after the initiation of fasting in the 4–1F and 2–2F/3–2F groups, as did the percentage of GFP^+ cells in BM and SP at 3 weeks post-fast (Fig. 2j). Analysis of WBC counts also showed that the fasting regimen reversed B-ALL progression (Fig. 2k). The fasted mice in the 4–1F and 3–2F groups had decreased leukemia burden rates as compared to control mice (Fig. 2l) and lived longer than did the control mice (Fig. 2m); whereas all control B-ALL mice were dead by day 58 after transplantation, more than 60% of the fasted mice survived more than 120 d. These results indicate that fasting at the middle-to-late stage of B-ALL is capable of reversing leukemia development.

To further evaluate how fasting impacts N-Myc-induced B-ALL development at a late stage of the disease, we tested the effects of the 2-IF/4–1F or 2–2F/3–2F fasting protocols in mice that received secondary transplantations (Fig. 2a). We found that the 4–1F or 3–2F fasting protocols inhibited B-ALL development in more than 40% of B-ALL mice at this very late stage. At 7 weeks after transplantation, the percentage of leukemic GFP^+ cells in PB, BM and SP, as well as WBC counts in PB, decreased significantly in fasted mice as compared to the fed controls (Fig. 2n,o). Moreover, the fasted mice had a lower percentage of $B220^+$ cells and a higher percentage of Mac-1^+ cells in the GFP^+ compartment than did controls (Supplementary Fig. 5), and had decreased leukemia burden rates and increased life spans (Fig. 2p,q), indicating that fasting inhibits B-ALL development in mice that have undergone secondary transplantations. We performed a similar set of experiments in the Notch1-induced T-ALL model and obtained similar results (Supplementary Fig. 6). Together, these results indicate that fasting blocks the development of B-ALL and T-ALL at both the tumor initiation stage and later stages of the disease.

Fasting induces rapid ALL differentiation and loss and upregulation of LEPR

To study the kinetics of fasting effects on ALL development, we fasted mice with B-ALL at the time at which leukemia had progressed to the mid-to-late-stage (~60% GFP^+ cells in PB). A single 48-h fast induced a significant reduction in the percentage of GFP^+ cells in PB, BM, SP and LV at day 2 and day 5 after the initiation of fasting (Fig. 3a,b). In fasted mice, the percentage of B220 cells decreased greatly in the GFP^+ leukemic cell compartment, but not in the GFP^- nonleukemic cell compartment (Fig. 3c and Supplementary Fig. 7a). GFP^+ leukemic cells had lower rates of apoptosis and proliferation than GFP^- cells in control mice; fasting increased apoptosis and proliferation rates in GFP^+

cells but decreased both in GFP^- cells (Fig. 3c and Supplementary Fig. 7b), indicating that ALL cells and nonleukemic cells respond differently to fasting treatment. Fasting did not have effects on levels of the senescence marker SA-β-gal in GFP^+ cells (Supplementary Fig. 7c). With respect to ALL cell differentiation, GFP^+ cells in fasted mice were more differentiated than those in control mice, with significantly increased expression of B cell maturation markers, including surface IgM, Ig κ and Ig λ, and reduced expression of immature B cell markers including terminal deoxynucleotidyl transferase (TDT) and surface CD43 (Fig. 3d). With respect to effects on metabolism, 48-h fasting (2F), 24-h fasting (1F) and two cycles of 24-h fasting (2–1F) showed similar effects, including a decrease in circulating glucose and insulin levels, lower levels of insulin-like growth factor (IGF)-1 and leptin in both PB and BM, and an increase in insulin-like growth factor binding protein 1 (IGFBP1) levels in both PB and BM. In many cases, these effects recovered to pre-fasting levels more slowly in the 2F and 2–1F conditions than in the 1F condition, an observation that is consistent with the severity of GFP^+ cell reduction in these regimens (Supplementary Fig. 7d–g). Fasting did not alter the homing properties of transplanted B-ALL cells, nor did fasting alter myeloid or lymphoid lineage distributions in the BM of wild-type mice (Supplementary Fig. 8). Taken together, these results indicate that fasting induces rapid differentiation and loss of ALL cells.

To study the underlying mechanisms, we collected GFP^+B220^+ B-ALL cells from control mice and from 1-d or 2-d fasted mice by flow cytometry for RNA-seq analysis. Consistent with the concept that fasting promotes B-ALL differentiation, the RNA-seq data indicated that the B cell terminal-differentiation program was initiated rapidly by fasting. The levels of mRNA or activity (as inferred by upstream regulator analysis in Ingenuity Pathway Analysis (IPA) tools) of most of the signature transcription factors of B cell terminal differentiation, including the key factors *Prdm1*, *Xbp1* and *Irf4* (refs. 28,29), were upregulated by fasting (Fig. 3e and Supplementary Table 1). Pathway analysis showed that the pathways of cytokine–cytokine receptor interaction, as well as the JAK–STAT pathway that acts downstream of cytokine receptors, were altered significantly; in particular, STAT3, a key player in the JAK–STAT pathway, was inferred to be highly activated by fasting (Fig. 3f and Supplementary Tables 2 and 3). Consistent with the inhibitory effects of fasting on N-Myc B-ALL and Notch1 T-ALL phenotypes, the inferred activities of N-Myc and Notch1, as well as the inferred activities of the oncogenes *Myc* and *Bcl3*, were reduced profoundly by fasting (Fig. 3f and Supplementary Table 3). Moreover, fasting reduced the protein levels of N-Myc in both B-ALL and T-ALL GFP^+ cells as compared to the fed condition (Supplementary Fig. 9). These results suggest that upregulation of cytokine-receptor signaling might be responsible for the inhibitory effects of fasting on ALL.

Consistent with this idea, we found that the expression levels of many cytokine receptors were upregulated in GFP^+B220^+ B-ALL cells from fasted mice (Fig. 3g). Among the cytokine receptors showing increased expression, we selected the leptin receptor (LEPR) as a candidate for mediating the antileukemic effects of fasting, on the basis of two criteria: its strong upregulation in cells from fasted mice and the negative $\log_2$ hazard ratio of its expression to survival rates of human patients with pre-B-ALL (that is, a positive correlation between LEPR expression level and overall survival) (Fig. 3g and Supplementary Table 4). Surface expression of LEPR on GFP^+ cells from fasted mice increased from day 1 to day 2

after fasting and was maintained thereafter (Fig. 3h). According to mRNA analysis, the long isoform of LEPR, *Ob-Rb*, was more highly expressed than the short isoform, *Ob-Ra* (Fig. 3i), and the level of *Ob-Rb* mRNA in leukemic cells was increased by fasting (Fig. 3j). Moreover, the levels of phospho-STAT3, the major effector of LEPR[30,31], were increased in leukemic cells by fasting (Fig. 3k). The fasting-induced increase in LEPR expression was more pronounced in leukemic GFP^+ $B220^+$ cells than in GFP^+ $B220^-$ cells, and these relative effects were reversed in nonleukemic GFP^- cell populations (Fig. 3l). *Ob-Rb* was also the more highly expressed isoform in T-ALL and AML cells, and the ratio of *Ob-Rb/Ob-Ra* expression in these cells was not affected by fasting (Supplementary Fig. 10a,b). Moreover, fasting induced rapid upregulation of surface LEPR levels in Notch-transformed T-ALL cells but not in MLL-AF9-transformed AML cells (Supplementary Fig. 10c). Notably, surface LEPR expression was lower on nonfasted B-ALL and T-ALL cells than on normal B and T lineage cells, respectively, whereas surface LEPR expression on AML cells was higher or equal to those on normal myeloid-lineage cells (Fig. 3m). Fasting did not alter the expression of surface LEPR on normal myeloid and lymphoid cells in nontumor bearing mice (Supplementary Fig. 10d), indicating that the effect of fasting on LEPR expression is specific to ALL cells. Taken together, these results demonstrate that fasting induces upregulation of LEPR and downstream signaling in ALL but not AML cells, which is consistent with the effects of fasting on leukemia development in these mouse models.

Fasting is known to reduce the level of plasma leptin[32], and adipocytokines have been proposed to affect tumor growth through local and micro-environmental regulation[33,34]. We found that fasting decreased the levels of not only circulating leptin, but also leptin in BM (Supplementary Fig. 7e,f). After fasting, the rate at which the leptin level returned to the pre-fasting level was slower in BM than in PB, and this effect was more pronounced in the 2F or 2–1F regimens than in the 1F regimen. The rate at which leptin levels recovered after fasting was concordant with the clearance rate of ALL cells (Supplementary Fig. 7e–g), which suggests that leptin might have roles in ALL inhibition at both the systemic and local levels. Moreover, the administration of leptin to B-ALL mice reversed fasting-induced upregulation of LEPR (Fig. 4a), which suggests that LEPR upregulation upon fasting occurs in response to leptin downregulation. Notably, the effect of fasting on decreasing the percentage of leukemic GFP^+ cells was partially but significantly rescued by leptin administration (Fig. 4a), suggesting that LEPR upregulation in ALL cells accounts for the antileukemic effects of fasting.

Attenuated LEPR signaling is essential for ALL development

To study the role of LEPR in the effects of fasting on leukemia development, we first used LEPR-deficient mice (hereafter $Lepr^{db/db}$ mice) to investigate whether attenuation of LEPR signaling is essential for ALL development[35,36]. Using these mice, we previously demonstrated that LEPR signaling promotes breast cancer development and metastasis through suppression of mitochondrial respiration[18,19]. We transplanted N-Myc-infected $Lepr^{+/+}$ and $Lepr^{db/db}$ BM Lin^- cells into wild-type recipient mice. As compared to mice transplanted with $Lepr^{+/+}$ cells, mice transplanted with $Lepr^{db/db}$ cells showed a significantly faster rise in the percentage of GFP^+ B-ALL cells and showed an increased percentage of GFP^+ cells in the PB, BM and SP, as well as increased WBC counts (Fig. 4b,c). Moreover,

within the GFP$^+$ compartment, B220$^+$ *Lepr*$^{db/db}$ cells arose more rapidly than B220$^+$*Lepr*$^{+/+}$ cells, and *Lepr*$^{db/db}$ cells showed a higher percentage of B220$^+$ CD43$^+$ precursors but a lower percentage of B220$^+$IgM$^+$ differentiated cells than B220$^+$ *Lepr*$^{+/+}$ cells (Fig. 4d,e). These results suggest that LEPR deficiency blocks the differentiation of B-ALL cells. Furthermore, *Lepr*$^{db/db}$ B-ALL mice had a significantly lower overall survival rate than control mice (Fig. 4f).

We also examined the effects of LEPR deficiency on T-ALL and AML development. Similarly to the situation in B-ALL, transplantation of *Lepr*$^{db/db}$ T-ALL cells led to faster leukemic progression as compared to transplantation of *Lepr*$^{+/+}$ T-ALL cells (Supplementary Fig. 11). By contrast, transplantation of *Lepr*$^{db/db}$ AML cells led to slightly slower leukemic progression than did the transplantation of *Lepr*$^{+/+}$ AML cells (Supplementary Fig. 12). These results suggest that LEPR negatively regulates ALL development but not AML development, which is consistent with the pattern of LEPR expression in ALL and AML cells.

Next, we used leptin-deficient (*Lep*$^{ob/ob}$) mice[19,37–39] or wild-type mice as the recipients of leukemic cell transplantation to test the effect of LEPR-ligand deficiency on B-ALL development. B-ALL developed faster in *Lep*$^{ob/ob}$ recipient mice than in wild-type mice (Supplementary Fig. 13a,b); moreover, the percentage of B220$^+$IgM$^+$ cells in the GFP$^+$ compartment was substantially lower in *Lep*$^{ob/ob}$ than in wild-type recipients, especially in the early stages of disease (Supplementary Fig. 13c), which suggests that B-ALL cells in *Lep*$^{ob/ob}$ mice are less differentiated than those in wild-type mice. *Lep*$^{ob/ob}$ B-ALL mice did not survive as long as wild-type mice (Supplementary Fig. 13d). The exacerbation of leukemia development in *Lep*$^{ob/ob}$ B-ALL mice was reversed by leptin administration (Supplementary Fig. 13a–d). By contrast, AML development was modestly delayed in *Lep*$^{ob/ob}$ recipient mice as compared to that in wild-type mice (Supplementary Fig. 14). Thus, the loss of leptin–LEPR signaling because of either LEPR deficiency in donor cells or leptin deficiency in recipient mice accelerates ALL development, consistent with the notion that attenuated LEPR expression is essential for ALL development.

LEPR is required for fasting-induced inhibition of ALL development

To determine whether LEPR is required for fasting-induced inhibition of ALL development, we transplanted *Lepr*$^{+/+}$ and *Lepr*$^{db/db}$ B220$^+$ B-ALL cells into WT recipient mice; once ~60% of cells in the PB were GFP$^+$, the mice were fasted for 48 h (Fig. 4g). In mice transplanted with *Lepr*$^{+/+}$ cells, fasting led to a drop in the percentage of GFP$^+$ cells in PB from 71.77 ± 6.15% pre-fasting to 1.16 ± 0.69% at day 2, followed by a rise to 2.93 ± 0.80% at day 3 and 63.47 ± 11.52% at day 5 (Fig. 4h). However, the same fasting regimen assigned to *Lepr*$^{db/db}$ B-ALL mice resulted in a significantly attenuated decrease in the percentage of GFP$^+$ cells in PB at days 2 and 3 (Fig. 4h). Moreover, whereas essentially all *Lepr*$^{+/+}$ B-ALL cells had differentiated into IgM$^+$ cells at days 2 and 3 after the initiation of fasting, *Lepr*$^{db/db}$ B-ALL cells did not undergo differentiation (Fig. 4i). These results indicate that a lack of LEPR in B-ALL cells confers resistance to fasting.

In parallel, we carried out a fasting regimen consisting of two cycles of 2-d fasting/2-d feeding at day 2 after transplantation (Fig. 4g). Similarly to the results with one 48-h fast,

LEPR deficiency in ALL cells resulted in the development of resistance by mouse recipients to the effects of two cycles of fasting (Fig. 4j–m). Mice transplanted with *Lepr*$^{db/db}$ T-ALL cells were also resistant to the antileukemic effects of both fasting regimens (Supplementary Fig. 15). Collectively, our results indicate that LEPR deficiency abrogates the fasting-induced block of ALL development, consistent with the idea that LEPR upregulation on ALL cells is responsible for the inhibitory effects of fasting on ALL.

LEPR induces ALL differentiation through PRDM1

To study how LEPR upregulation might inhibit ALL, we overexpressed LEPR in B-ALL cells. LEPR overexpression significantly elevated the expression of surface IgM and light chains λ and κ, and significantly decreased TdT expression, indicating that LEPR induces B-ALL differentiation (Fig. 5a). Among the key transcription factors required to activate B cell terminal differentiation[28,29], LEPR overexpression significantly upregulated the mRNA and protein levels of XBP1, and especially, PRDM1 (Fig. 5b,c and Supplementary Fig. 16a), although no changes in their mRNA levels were observed in B220^{+} BM cells of ob/ob or db/db mice (Supplementary Fig. 16b). PRDM1 expression can be activated by STAT3 and STAT5 (ref. 28), which are major effectors of LEPR signaling[30,31]. In addition to its role in B cell terminal differentiation, PRDM1 is also a crucial factor for the differentiation of terminal effector T cells, and the gene encoding PRDM1 is a tumor-suppressor gene in lymphoid malignancies[28,40,41]. Knockdown of *Prdm1* reversed *Lepr* induced B-ALL differentiation *in vitro* (Fig. 5d and Supplementary Fig. 16c), which suggests that PRDM1 mediates the effect of LEPR on the promotion of ALL cell differentiation.

Next, we overexpressed LEPR (the *Ob-Rb* isoform) in mouse B-ALL cells (BM cells of mice transplanted with *N-Myc*-expressing fetal liver cells), and followed up with secondary transplantation. LEPR overexpression significantly inhibited B-ALL development, as evidenced by decreases in the percentage of GFP^{+} cells and WBC counts, increased B-ALL cell differentiation and a prolongation of mouse survival as compared to the control vector (Fig. 5e–h). By contrast, LEPR overexpression had little effect on MLL-AF9-driven AML development (Supplementary Fig. 17). Similarly to LEPR overexpression, PRDM1 overexpression in mouse B-ALL cells significantly inhibited B-ALL development (Fig. 5i–l). Additionally, we co-expressed shRNAs targeting *Prdm1* with *Lepr* in mouse B-ALL cells, and found that *Prdm1* knockdown blocked the ability of *Lepr* overexpression to inhibit B-ALL (Fig. 5m–p). This rescue experiment confirms that PRDM1 has an important role downstream of LEPR in regulating B-ALL development.

We also tested the effects of LEPR overexpression when co-infected with N-Myc in primary fetal liver cells. In this setting, LEPR overexpression abrogated B-ALL development (Supplementary Fig. 18a and b). As a control, mice transplanted with LEPR-infected normal fetal liver cells showed only modest changes in myeloid and lymphoid cell percentages (Supplementary Fig. 18c). Little variation in the distribution of these lineages was observed between wild-type and LEPR-deficient (db/db) mice under either fed or fasted conditions (Supplementary Fig. 18d), and the distribution of these lineages was not substantially affected in the nonleukemic GFP^{-} cell compartment of mice transplanted with either *Lepr*$^{+/+}$ or *Lepr*$^{db/db}$ B-ALL or T-ALL cells (Supplementary Fig. 18e).

Fasting and *LEPR* signaling inhibit human ALL development

To study the importance of LEPR in human leukemia development, we first performed an *in silico* analysis of *LEPR* mRNA expression in more than 2,000 human leukemia and normal BM samples (GSE13159). *LEPR* was expressed at significantly lower levels in all types of lymphoid leukemia cells tested as compared to normal BM samples, whereas *LEPR* was expressed at similar levels in normal and myeloid-leukemia cells (Fig. 6a). Consistent with these findings, flow cytometry analysis showed that human B-ALL and T-ALL cells, but not AML cells, expressed significantly less cell surface LEPR than did their normal cell counterparts (Fig. 6b). Moreover, pediatric patients with pre-B-ALL with higher *LEPR* mRNA expression tended to survive longer than those with lower levels (although this was not a significant effect) (Children's Oncology Group clinical trial P9906), whereas there was no such correlation in patients with AML (The Cancer Genome Atlas) (Fig. 6c). These results suggest a conserved role of attenuated LEPR expression in supporting of human ALL development.

LEPR sensitivity can be affected by *LEPR* gene polymorphism[42,43], which would not be detected in microarray experiments. To further study the role of LEPR signaling in human leukemia, we expanded the survival analysis to all known LEPR-signaling-related genes[44]. We found that the expression patterns of 29 out of 118 LEPR-signaling-related genes (24.6%) were significantly correlated with pediatric pre-B-ALL overall or event-free survival; this correlation was significantly higher than that for LEPR-signaling-unrelated genes (2,846 out of 20,933, 13.6%) (Fig. 6d). By contrast, there was no significant difference between the correlation of LEPR-signaling-related and LEPR-signaling-unrelated genes with the overall survival of patients with AML (Fig. 6d). Furthermore, among the 29 genes whose expression was significantly correlated with the outcome of patients with pre-B-ALL, most of the genes that negatively regulate or are negatively regulated by LEPR signaling showed a correlation with poor outcome, whereas genes that positively regulate or are positively regulated by LEPR signaling showed a correlation with better outcome (Fig. 6e and Supplementary Table 5). These results indicate that LEPR signaling is positively correlated with survival in human pre-B-ALL but not in AML.

Next, we determined the effect of fasting on human ALL development *in vivo* by using a xenograft model. After showing that fasting inhibited N-Myc-driven B-ALL development in sub-lethally irradiated *scid* recipient mice (Supplementary Fig. 19), we tested the effects of fasting in sub-lethally irradiated *scid* mice bearing xenografts of human pre-B-ALL cell line NALM-6. Fasting increased LEPR expression on NALM-6 cells as compared to that in the fed condition (Fig. 6f). All fed control mice displayed paraplegia and died of disseminated leukemia by day 35. However, in mice that were fasted with a regimen consisting of three cycles of 2-d fasting/2-d feeding, initiated on day 2 after the cells were injected, the incidence of paraplegia was markedly reduced, the percentage of $hCD19^{+}$NALM-6 cells was significantly decreased in BM and SP and overall survival was significantly improved as compared to controls (Fig. 6g–i). These data indicate that fasting effectively inhibits the development of human ALL in the xenograft mouse model.

DISCUSSION

Dietary restriction is associated with positive therapeutic outcome in both animal models and humans, and it selectively suppresses certain solid tumor types, especially when combined with chemotherapy[1–6]. Here, by using mouse models of N-Myc B-ALL, Notch-1 T-ALL, MLL-AF9 AML and AML1-Eto9a AML, as well as a xenograft mouse model of human leukemia, we demonstrated that fasting alone greatly inhibits the development of ALL but not AML, and we identified the underlying mechanism responsible for the differing response to fasting treatment. Our results indicate that the effects of fasting on leukemia development are cancer-type dependent and reveal the importance of attenuated LEPR signaling in ALL development and maintenance.

In most human populations, there is a strong association between obesity and ALL leukemia, but the underlying mechanisms remain poorly understood[45–47]. Patients with obesity and ALL have worse outcomes[46,48] than patients with ALL but without obesity, and patients with ALL have a high risk of obesity after treatment[42,49]. In addition, diet-induced obesity can accelerate the development of ALL in mouse models[50]. Obesity is characterized by leptin resistance that is usually marked by elevated leptin levels but attenuated LEPR signaling[51]. Here we demonstrated the importance of attenuated LEPR expression in ALL development and showed that LEPR signaling correlates with pre-B-ALL patient outcome. Our study suggests a possible link between obesity, LEPR signaling and ALL development. Adipocytes protect ALL cells from chemotherapy and promote relapse[46,52]. We suggest that adipocytes can provide a niche-like environment for ALL cells in which there are high leptin levels, which leads to the suppression of LEPR expression and thereby the inhibition of ALL cell differentiation.

A key finding of our study is that fasting leads to increased LEPR signaling and subsequent inhibition of ALL development, but further study of the underlying mechanisms is needed. In particular, the mechanism by which fasting induces upregulation of LEPR expression and signaling is not yet clear. We speculate that a reduction in systemic leptin levels by fasting leads to a compensatory elevation of LEPR expression on leukemia cells. A similar induction of *LEPR* mRNA and LEPR protein levels by fasting has been well documented in the nervous system[53]. The very low level of LEPR in nonfasted ALL cells suggests that LEPR expression levels are the limiting factor in leptin LEPR signaling, such that fasting-induced elevation of LEPR levels would increase signaling, despite a drop in circulating leptin levels. This situation might be specific to ALL cells that express very low levels of LEPR, as compared to other types of cells, including AML cells that express relatively high levels of LEPR.

It will be important to determine whether ALL cells can become resistant to the effects of fasting, which might provide more insights into leukemia pathogenesis. In addition, although both N-Myc B-ALL and Notch-1 T-ALL models might depend on Myc for the leukemia phenotype[54], the MLL-AF9- and *AML1-Eto9a*- AML models do not. This raises an interesting possibility that fasting might affect leukemia development based on specific oncogenes, such as *Myc*. Future studies are warranted to define more precisely whether differences in the cell of origin or in oncogene drivers contribute to the differential responses

of ALL and AML to fasting. Moreover, aside from LEPR signaling, other systemic and leukemic cell effects will undoubtedly be involved in the inhibitory effects of fasting on ALL. For example, the growth hormone (GH)–GH receptor (GHR)–IGF-1 axis has an important role in the treatment of certain solid tumors by a combination of fasting and chemotherapy[5,10]. Notably, the GH–GHR pathway shares common JAK–STAT downstream targets with the leptin–LEPR pathway[5]. Whether these pathways work separately or cooperatively in mediating the effects of fasting on different tumor should be further investigated.

Although the therapeutic strategy of forcing malignant cells to terminally differentiate was proposed several decades ago[55], differentiation therapy has so far been used successfully only in a subtype of AML, acute promyelocytic leukemia (APL)[56,57]. Our data show that fasting can effectively induce B-ALL differentiation at both the early and later stages of disease, which suggests the potential of fasting for differentiation therapy in patients with *de novo* and relapsed ALL. Our study also provides a platform for identifying new targets for ALL treatment.

METHODS

Methods, including statements of data availability and any associated accession codes and references, are available in the online version of the paper.

ONLINE METHODS

Mice.

C57BL/6 mice were purchased from the University of Texas Southwestern Medical Center animal-breeding core facility. Leptin-deficient mice (B6.Cg-*Lep*^{ob}/J), *LEPR*-deficient mice (B6.BKS(D)-*LEPR*^{db}/J), and BALB *scid* mice were purchased from the Jackson Laboratory. Mice were maintained at the University of Texas Southwestern Medical Center animal facility and at Binzhou Medical University. All animal experiments were performed with the approval of the UT Southwestern Committee on Animal Care and the approval of Binzhou Medical University Committee on Animal Care. For each experiment, the same sex of mice 6–8 weeks of age were used and randomly allocated to each group. The minimum number of mice in each group was calculated by using the ‘cpower’ function in R/Hmisc package.

Cell culture.

293T cells were cultured in Dulbecco’s modified Eagle’s medium (DMEM) supplemented with 10% FBS at 37 °C in 5% CO_2. Primary mouse B-ALL cells were cultured in IMDM supplemented with 10 ng/ml recombinant mouse Il-7 (Peprotech) on OP9 stromal cells. Primary mouse AML cells were cultured in serum-free stemspan (Stemcell techonologies) supplemented with 10 ng/ml SCF (Peprotech). The human leukemia cell line NALM-6 (DSMZ, ACC128) was cultured in RPMI-1640 supplemented with 10% FBS at 37 °C in 5% CO_2. NALM-6 cells display a $CD3^-/CD19^+$ phenotype by antibody staining and are able to induce B-ALL when xenografted into *scid* mice[58,59]. All cell lines were routinely tested using a mycoplasma-contamination kit (R&D). Primary human AML samples were obtained from the tissue bank at the University of Texas Southwestern Medical Center. Informed

consent was obtained under a protocol reviewed and approved by the Institutional Review Board at the University of Texas Southwestern Medical Center. Samples were frozen in FBS (FBS) with 10% DMSO and stored in liquid nitrogen.

Virus construction and infection.

For retrovirus packaging, the retroviral constructs MSCV-Notch1-IRES-GFP (T-ALL)[24], MSCV-MLL-AF9-IRES-YFP (AML)[25,26], pMXs-N-Myc-IRES-GFP (B-ALL)[23], MSCV-*LEPR*, MSCV-*LEPR*-DsRed, or MSCV-PRDM1-IRES-DsRed were mixed with PCL-ECO (2:1), followed by transfection into 293T cells using Lipofectamine 2000 (Invitrogen). For lentivirus packaging, pLentiLox3.7-based shRNA constructs were mixed with psPAX2 and pMD2.G (Addgene) at a ratio of 4:3:1 and transfected into 293T cells using Lipofectamine 2000 (Invitrogen). Virus-containing supernatant was collected 48–72 h post-transfection and used for spin infection as described previously[16,17]. Briefly, the virus supernatant was collected and filtered through a 0.45-mm filter. For infection of Lin^- cells from BM or fetal liver, Lin^- cells were suspended in virus supernatant supplemented with 4 μg/ml polybrene at 10^6/ml and placed in six-well plate for spin infection (900*g*, 90 min at 37 °C). For infection of mouse B-ALL and AML cells, the virus was concentrated by centricon centrifugal filters (EMD Millipore), and loaded onto retronectin (50 μg/ml, Clontech) coated six-well petri plates by centrifugation (2,000*g*, 90 min, 37 °C). After removing the supernatant, 2×10^6 cells per well were added for centrifugation at 600*g* for 30 min.

Leukemia transplantation and fasting.

Lin^- cells were isolated from the fetal liver or bone marrow of wild-type mice or littermate LEPR-deficient or WT mice, and infected with oncogene-IRES-GFP(YFP) expressing retrovirus. Infected mouse Lin^- cells (300,000) were transplanted into lethally irradiated (900 cGy) C57BL/6 mice or leptin-deficient mice (6–8 weeks old) by retro-orbital injection. For the second transplantation step, we used FACS to isolate GFP^+ or YFP^+ BM cells from primary recipient mice and transplanted 3,000 cells (AML) or 10,000 cells (B- or T-ALL) together with 3×10^5 normal BM cells into lethally irradiated recipients.

According to our approved protocols, one to six 1-d fasting/1-d feeding cycles or one to four 2-d fasting/2-d feeding cycles were performed at day 2 after transplantation or at mid-stage of leukemia development (around 3–4 weeks after transplantation). For *in vivo* leptin administration during 48-h fasting, mouse recombinant leptin (R&D system, 5 μg/15 g body weight) or control PBS was retro-orbitally injected into mice daily during fasting.

Human AML xenograft and fasting.

Xenografting was performed essentially as we have previously described[20,60]. Briefly, adult *scid* mice (6–8 weeks old) were sub-lethally irradiated with 250 cGy total body irradiation before transplantation. Either 5×10^6 pre-B-ALL NALM-6 cells were used per mouse for retro-orbital injection. At 3–6 weeks after transplantation, the PB, BM, spleen and liver were assessed for engraftment. For fasting, mice were fasted with up to four cycles of 1-d fasting/1-d feeding.

Leukemia characterization.

We performed the procedure as we have previously described[16,17]. After transplantation, we monitored the survival, examined the size and histological properties of BM, spleen, and liver and analyzed the numbers and infiltration of leukemia cells in PB, BM, spleen, and liver. WBC counts in PB were measured using a Hemavet 950FS. We also characterized different populations of leukemia cells using flow cytometry. Leukemia characterization was performed by investigators blinded to the experimental groups. Moribund leukemic mice were euthanized and the time was recorded as the time of death. Mice that died for reasons unrelated to leukemia within 10 d after transplantation were excluded from the data analysis.

Flow cytometry.

For flow cytometry analyses of mouse PB, BM and SP, leukemia cells were stained with anti-Mac-1-APC (rat, M1/70, 1:200 dilution), anti-Gr-1-PE (rat, RB6–8C5, 1:200 dilution), anti-CD3-APC (hamster, 145–2C11, 1:200 dilution), anti-B220-PE (rat, RA3–6B2, 1:200 dilution), anti-Kit-PE (rat, 2B8, 1:200 dilution) monoclonal antibodies (BD Pharmingen), anti-CD4 (rat, RM4–5, Biolegend), anti-CD8, anti-CD43 (rat, S7, 1:200 dulution, BD Pharmingen), anti-CD19 (rat, 1D3, 1:200 dilution, eBioscience), anti-IgM (rat, II/41, 1:200 dilution, BD Pharmingen), anti-IgD (rat, 11–26c, 1:200 dilution, eBioscience), anti-Igk (rat, 187.1, 1:200 dilution, BD Pharmingen), anti-Igl (rat, R26–46, 1:200 dilution, BD Pharmingen), or anti-*LEPR*-biotin (goat polyclonal antibody, 1:50 dilution, R&D system) followed by streptavidin-APC or streptavidin-PE-Cy5.5 (1:200 dilution, BD Pharmingen). Human patient samples were stained with anti-human CD19-PE (mouse, HIB19, 1:50 dilution, eBioscience), anti-human CD3-PE (mouse, HIT3a, 1:50 dilution eBioscience), anti-human CD33 (mouse, HIM3–4, 1:20 dilution, eBioscience), anti-human CD45 (mouse, HI30, 1:50 dilution, BD Pharmingen), anti-human CD34 (mouse, 4H11, 1:50 dilution, eBioscience), anti-human CD4 (mouse, OKT4, 1:50 dilution, eBioscience), anti-human CD8a (mouse, 1:20 dilution, R&D system), anti-human CD40 (mouse, 5C3, 1:20 dilution, BioLegend), anti-human IgM (mouse, SA-DA4, 1:20 dilution, eBioscience), anti-human IgD (mouse, IA6–2, 1:20 dilution, eBioscience), or anti-human *LEPR* (mouse, 52263, 1:50 dilution) monoclonal antibodies (BD Pharmingen). Intracellular staining of Ki67 (rat SolA15, 1:200 dilution, eBioscience) and PRDM1 (rat, 6D3, 1:50 dilution, BD pharmingen) or pSTAT3 (mouse, LUVNKLA, 1:20 dilution, eBioscience) was performed using the Foxp3/Transcription factor staining set (eBioscience) or Fixation/Methanol protocol (eBioscience) provided by the manufacturers. For analysis of human hematopoietic engraftment in *scid* mice, we followed our previously published protocol[20,60] and used anti-human CD19 (BD Pharmingen) and anti-human CD45-PE (mouse, HI30, BD Pharmingen, 1:50 dilution) to quantify total human AML engraftment.

Colony assays.

Mouse AML cells were diluted to the indicated concentration in IMDM with 2% FBS and were then seeded into methylcellulose medium M3534 (StemCell Technologies) for myeloid colony formation analysis, as described previously[16,17].

Plasmid construction.

The MSCV-IRES-DsRed plasmid was constructed by replacing GFP with DsRed in the MSCV-IRES-GFP plasmid (Addgene). Mouse *LEPR* and PRDM1, obtained by PCR from mouse bone marrow cDNA, were used to construct the MSCV-*LEPR*, MSCV-*LEPR*-IRES-DsRed and MSCV-PRDM1-IRES-DsRed plasmids. pLentiLoxp3.7 (Addgene) was modified by replacing the GFP reporter with DsRed, and used to construct PRDM1 shRNA expressing lentiviral vectors. The target sequences for shPRDM1–1 and shPRDM1–2 were 5′ GGGTGGTTCGGTCCTGTATTCT 3′ and 5′ ATGT ACTCCTTACTTACCACG 3′, respectively.

Quantitative RT–PCR.

Total RNA was extracted using RNAeasy kit (QIAGEN) and reverse transcribed into cDNA using SuperScript III Reverse Transcriptase (Invitrogen) according to the protocol provided. Real-time PCR was performed with the primers listed in Supplementary Table 6 using SYBR Green Master Mix (Bio-Rad). mRNA levels were normalized to the level of *GAPDH* RNA transcripts present in the same sample.

Western blotting.

Cells were lysed in Laemmli sample buffer (Sigma-Aldrich) supplemented with protease inhibitor cocktail (Roche Diagnostics). Samples were separated on SDS–PAGE gels (Bio-Rad) and transferred on nitrocellulose membranes (Bio-Rad) for protein detection as described[16,17]. Primary antibodies including anti-PRDM1 (eBioscience, 6D3, 1:200), anti-XBP-1s (Biolegend, 9D11A43, 1:500), anti-N-Myc (Santa Cruz, sc-53993, 1:500) and anti-Myc (Santa Cruz, sc-40, 1:500), as well as horseradish peroxidase (HRP) conjugated secondary antibodies (R&D system, HAF007, 1:1,000, and HAF005, 1:1,000) and chemi-luminescent substrate (Invitrogen), were used.

RNA-seq analysis.

RNA was purified from sorted cells with Qiagen RNeasy Mini Kit and then reverse-transcribed with SuperScript III Reverse Transcriptase (Invitrogen) according to the manufacturer's instructions. RNA-seq was performed at the UTSW Genomics and Microarray Core Facility. The cDNA was sonicated using a Covaris S2 ultrasonicator, and libraries were prepared with the KAPA High Throughput Library Preparation Kit. Samples were end-repaired and the 3′ ends were adenylated and barcoded with multiplex adapters. PCR-amplified libraries were purified with AmpureXP beads and validated on the Agilent 2100 Bioanalyzer. Before being normalized and pooled, samples were quantified by Qubit (Invitrogen) and then run on an Illumina Hiseq 2500 instrument using PE100 SBS v3 reagents to generate 51-bp single-end reads. Before mapping, reads were trimmed to remove low-quality regions in the ends. Trimmed reads were mapped to the mouse genome (mm10) using TopHat v2.0.1227 with the UCSC iGenomes GTF file from Illumina.

Methods for data normalization and analysis are based on the use of "internal standards"[61] that characterize some aspects of the system's behavior, such as technical variability, as presented elsewhere[62,63]. Genes with $\log_2$ (fold change) > 2, $P < 0.05$ and RPKM > 0.5 were deemed to be significantly differentially expressed between the two conditions, and used for

pathway analysis and upstream transcription factor analysis. Pathway analysis was conducted using the Consensus-Path-DB database (http://cpdb.molgen.mpg.de/CPDB)[64]. Upstream transcription-factor analysis was conducted using QIAGEN's Ingenuity tool (http://www.ingenuity.com/)[65]. Gene heat maps were clustered by hierarchical clustering (hclust function in R, http://www.r-project.org).

In silico analyses and survival analysis.

Microarray data of human leukemia patients were obtained from the GEO data set accession number GSE13159. *LEPR* expression levels were calculated by averaging the values from probe sets that recognize all *LEPR* isoforms (211354_s_at, 211355_x_at, 211356_x_at). For survival analyses, AML and ALL data were obtained from the National Cancer Institute TCGA AML database (https://tcga-data.nci.nih.gov/tcga) and National Cancer Institute TARGET Data Matrix of the Children's Oncology Group (COG) Clinical Trial P9906 (ftp://caftpd.nci.nih.gov/pub/dcc_target/ALL/Phase_I/Discovery/clinical/), respectively. Patients were divided into two groups at the 50th percentile according the level of a probe set or a gene (average of multiple probe sets of a gene); for *LEPR*, we used the probe sets recognizing all *LEPR* isoforms (211354_s_at, 211355_x_at, 211356_x_at). Kaplan–Meier survival analysis was used to estimate overall survival and a log–rank test was used to compare survival differences between patient groups using R software.

Statistical analyses.

Statistical analysis was done using Microsoft Excel, Prism 5.0 (Graphpad) and R software. Data were analyzed by Student's *t*-test or χ-squared test and were considered to be statistically significant if $P < 0.05$. A variance similarity test (f-test) was performed before the *t*-test. All *t*-tests and χ-squared tests were two-tailed unless otherwise indicated. The survival rates of the two groups were analyzed using a log–rank test and were considered to be statistically significant if $P < 0.05$.

Data-availability statement.

RNA-seq data have been deposited in Gene Expression Omnibus under accession number GSE89622.

Supplementary Material

Refer to Web version on PubMed Central for supplementary material.

ACKNOWLEDGMENTS

We would like to acknowledge the support by grants from the US National Institutes of Health 1R01CA172268 (C.C.Z.), Leukemia & Lymphoma Society Awards 1024-14 (C.C.Z.) and TRP-6024-14 (C.C.Z.), CPRIT RP140402 (C.C.Z.), 1R01HL089966 (L.J.H.), R01-DK55758 (P.E.S.) and RP140412 (P.E.S.).

References

1. Hursting SD, Lavigne JA, Berrigan D, Perkins SN & Barrett JC Calorie restriction, aging, and cancer prevention: mechanisms of action and applicability to humans. Annu. Rev. Med 54, 131–152 (2003). [PubMed: 12525670]

2. Fontana L & Partridge L Promoting health and longevity through diet: from model organisms to humans. Cell 161, 106–118 (2015). [PubMed: 25815989]
3. Mihaylova MM, Sabatini DM & Yilmaz OH Dietary and metabolic control of stem cell function in physiology and cancer. Cell Stem Cell 14, 292–305 (2014). [PubMed: 24607404]
4. Bordone L & Guarente L Calorie restriction, SIRT1 and metabolism: understanding longevity. Nat. Rev. Mol. Cell Biol 6, 298–305 (2005). [PubMed: 15768047]
5. Longo VD & Mattson MP Fasting: molecular mechanisms and clinical applications. Cell Metab. 19, 181–192 (2014). [PubMed: 24440038]
6. Kalaany NY & Sabatini DM Tumours with PI3K activation are resistant to dietary restriction. Nature 458, 725–731 (2009). [PubMed: 19279572]
7. Di Biase S et al. Fasting-mimicking diet reduces HO-1 to promote T cell-mediated tumor cytotoxicity. Cancer Cell 30, 136–146 (2016). [PubMed: 27411588]
8. Pietrocola F et al. Caloric restriction mimetics enhance anticancer immunosurveillance. Cancer Cell 30, 147–160 (2016). [PubMed: 27411589]
9. Cheng CW et al. Prolonged fasting reduces IGF-1/PKA to promote hematopoietic-stem-cell-based regeneration and reverse immunosuppression. Cell Stem Cell 14, 810–823 (2014). [PubMed: 24905167]
10. Lee C et al. Fasting cycles retard growth of tumors and sensitize a range of cancer cell types to chemotherapy. Sci. Transl. Med 4, 124ra27(2012).
11. Döhner H, Weisdorf DJ & Bloomfield CD Acute myeloid leukemia. N. Engl. J. Med 373, 1136–1152 (2015). [PubMed: 26376137]
12. Inaba H, Greaves M & Mullighan CG Acute lymphoblastic leukaemia. Lancet 381, 1943–1955 (2013). [PubMed: 23523389]
13. Ntziachristos P, Lim JS, Sage J & Aifantis I From fly wings to targeted cancer therapies: a centennial for notch signaling. Cancer Cell 25, 318–334 (2014). [PubMed: 24651013]
14. Kocabas F et al. Meis1 regulates the metabolic phenotype and oxidant defense of hematopoietic stem cells. Blood 120, 4963–4972 (2012). [PubMed: 22995899]
15. Simsek T et al. The distinct metabolic profile of hematopoietic stem cells reflects their location in a hypoxic niche. Cell Stem Cell 7, 380–390 (2010). [PubMed: 20804973]
16. Zheng J et al. Inhibitory receptors bind ANGPTLs and support blood stem cells and leukaemia development. Nature 485, 656–660 (2012). [PubMed: 22660330]
17. Kang X et al. The ITIM-containing receptor LAIR1 is essential for acute myeloid leukaemia development. Nat. Cell Biol 17, 665–677 (2015). [PubMed: 25915125]
18. Park J, Euhus DM & Scherer PE Paracrine and endocrine effects of adipose tissue on cancer development and progression. Endocr. Rev 32, 550–570 (2011). [PubMed: 21642230]
19. Park J, Kusminski CM, Chua SC & Scherer PE Leptin receptor signaling supports cancer cell metabolism through suppression of mitochondrial respiration in vivo. Am. J. Pathol 177, 3133–3144 (2010). [PubMed: 21056997]
20. Zheng J et al. Ex vivo expanded hematopoietic stem cells overcome the MHC barrier in allogeneic transplantation. Cell Stem Cell 9, 119–130 (2011). [PubMed: 21816363]
21. Zheng J et al. Profilin 1 is essential for retention and metabolism of mouse hematopoietic stem cells in bone marrow. Blood 123, 992–1001 (2014). [PubMed: 24385538]
22. Deng M et al. A motif in LILRB2 critical for Angptl2 binding and activation. Blood 124, 924–935 (2014). [PubMed: 24899623]
23. Sugihara E et al. Ink4a and Arf are crucial factors in the determination of the cell of origin and the therapeutic sensitivity of Myc-induced mouse lymphoid tumor. Oncogene 31, 2849–2861 (2012). [PubMed: 21986948]
24. Weng AP et al. Activating mutations of NOTCH1 in human T cell acute lymphoblastic leukemia. Science 306, 269–271 (2004). [PubMed: 15472075]
25. Krivtsov AV et al. Transformation from committed progenitor to leukaemia stem cell initiated by MLL-AF9. Nature 442, 818–822 (2006). [PubMed: 16862118]
26. Somervaille TC & Cleary ML Identification and characterization of leukemia stem cells in murine MLL-AF9 acute myeloid leukemia. Cancer Cell 10, 257–268 (2006). [PubMed: 17045204]

27. Yan M et al. A previously unidentified alternatively spliced isoform of t(8;21) transcript promotes leukemogenesis. Nat. Med 12, 945–949 (2006). [PubMed: 16892037]
28. Shapiro-Shelef M & Calame K Regulation of plasma-cell development. Nat. Rev. Immunol 5, 230–242 (2005). [PubMed: 15738953]
29. Shi W et al. Transcriptional profiling of mouse B cell terminal differentiation defines a signature for antibody-secreting plasma cells. Nat. Immunol 16, 663–673 (2015). [PubMed: 25894659]
30. Vaisse C et al. Leptin activation of Stat3 in the hypothalamus of wild-type and ob/ob mice but not db/db mice. Nat. Genet 14, 95–97 (1996). [PubMed: 8782827]
31. Morris DL & Rui L Recent advances in understanding leptin signaling and leptin resistance. Am. J. Physiol. Endocrinol. Metab 297, E1247–E1259 (2009). [PubMed: 19724019]
32. Weigle DS et al. Effect of fasting, refeeding, and dietary fat restriction on plasma leptin levels. J. Clin. Endocrinol. Metab 82, 561–565 (1997). [PubMed: 9024254]
33. Andò S & Catalano S The multifactorial role of leptin in driving the breast cancer microenvironment. Nat. Rev. Endocrinol 8, 263–275 (2011). [PubMed: 22083089]
34. Khandekar MJ, Cohen P & Spiegelman BM Molecular mechanisms of cancer development in obesity. Nat. Rev. Cancer 11, 886–895 (2011). [PubMed: 22113164]
35. Chua SC Jr. et al. Phenotypes of mouse diabetes and rat fatty due to mutations in the OB (leptin) receptor. Science 271, 994–996 (1996). [PubMed: 8584938]
36. Chen H et al. Evidence that the diabetes gene encodes the leptin receptor: identification of a mutation in the leptin receptor gene in db/db mice. Cell 84, 491–495 (1996). [PubMed: 8608603]
37. Coleman DL & Hummel KP The influence of genetic background on the expression of the obese (Ob) gene in the mouse. Diabetologia 9, 287–293 (1973). [PubMed: 4588246]
38. Zhang Y et al. Positional cloning of the mouse obese gene and its human homologue. Nature 372, 425–432 (1994). [PubMed: 7984236]
39. Fantuzzi G & Faggioni R Leptin in the regulation of immunity, inflammation, and hematopoiesis. J. Leukoc. Biol 68, 437–446 (2000). [PubMed: 11037963]
40. Boi M, Zucca E, Inghirami G & Bertoni F PRDM1/BLIMP1: a tumor suppressor gene in B and T cell lymphomas. Leuk. Lymphoma 56, 1223–1228 (2015). [PubMed: 25115512]
41. Hangaishi A & Kurokawa M Blimp-1 is a tumor suppressor gene in lymphoid malignancies. Int. J. Hematol 91, 46–53 (2010). [PubMed: 20047096]
42. Ross JA et al. Genetic variation in the leptin receptor gene and obesity in survivors of childhood acute lymphoblastic leukemia: a report from the Childhood Cancer Survivor Study. J. Clin. Oncol 22, 3558–3562 (2004). [PubMed: 15337805]
43. Wheeler E et al. Genome-wide SNP and CNV analysis identifies common and low-frequency variants associated with severe early-onset obesity. Nat. Genet 45, 513–517 (2013). [PubMed: 23563609]
44. Vishalakshi N et al. A comprehensive curated reaction map of leptin Signaling Pathway. J. Proteomics Bioinform 4, 184–189 (2011).
45. Teras LR et al. in Energy Balance and Hematologic Malignancies Vol. 5 1st edn. (eds. Mittelman SD & Berger NA) 1–69 (Springer, New York, 2012).
46. Sheng X & Mittelman SD The role of adipose tissue and obesity in causing treatment resistance of acute lymphoblastic leukemia. Front Pediatr. 2, 53(2014). [PubMed: 24926474]
47. Bifulco M & Malfitano AM Comment on “the negative impact of being underweight and weight loss on survival of children with acute lymphoblastic leukemia.”. Haematologica 100, e118–e119 (2015). [PubMed: 25740108]
48. Butturini AM et al. Obesity and outcome in pediatric acute lymphoblastic leukemia. J. Clin. Oncol 25, 2063–2069 (2007). [PubMed: 17513811]
49. Oeffinger KC et al. Obesity in adult survivors of childhood acute lymphoblastic leukemia: a report from the Childhood Cancer Survivor Study. J. Clin. Oncol 21, 1359–1365 (2003). [PubMed: 12663727]
50. Yun JP et al. Diet-induced obesity accelerates acute lymphoblastic leukemia progression in two murine models. Cancer Prev. Res. (Phila.) 3, 1259–1264 (2010). [PubMed: 20823291]

51. Myers MG Jr., Leibel RL, Seeley RJ & Schwartz MW Obesity and leptin resistance: distinguishing cause from effect. Trends Endocrinol. Metab 21, 643–651 (2010). [PubMed: 20846876]
52. Pramanik R, Sheng X, Ichihara B, Heisterkamp N & Mittelman SD Adipose tissue attracts and protects acute lymphoblastic leukemia cells from chemotherapy. Leuk. Res 37, 503–509 (2013). [PubMed: 23332453]
53. Baskin DG et al. Increased expression of mRNA for the long form of the leptin receptor in the hypothalamus is associated with leptin hypersensitivity and fasting. Diabetes 47, 538–543 (1998). [PubMed: 9568684]
54. Weng AP et al. c-Myc is an important direct target of Notch1 in T-cell acute lymphoblastic leukemia/lymphoma. Genes Dev. 20, 2096–2109 (2006). [PubMed: 16847353]
55. Nowak D, Stewart D & Koeffler HP Differentiation therapy of leukemia: 3 decades of development. Blood 113, 3655–3665 (2009). [PubMed: 19221035]
56. Efficace F et al. Randomized phase III trial of retinoic acid and arsenic trioxide versus retinoic acid and chemotherapy in patients with acute promyelocytic leukemia: health-related quality-of-life outcomes. J. Clin. Oncol 32, 3406–3412 (2014). [PubMed: 25245446]
57. Lo-Coco F et al. Retinoic acid and arsenic trioxide for acute promyelocytic leukemia. N. Engl. J. Med 369, 111–121 (2013). [PubMed: 23841729]
58. Hurwitz R et al. Characterization of a leukemic cell line of the pre-B phenotype. Intl. J. Cancer. Journal international du cancer 23, 174–180 (1979).
59. Filshie R, Gottlieb D & Bradstock K VLA-4 is involved in the engraftment of the human pre-B acute lymphoblastic leukaemia cell line NALM-6 in SCID mice. Br. J. Haematol 102, 1292–1300 (1998). [PubMed: 9753059]
60. Zhang CC, Kaba M, Iizuka S, Huynh H & Lodish HF Angiopoietin-like 5 and IGFBP2 stimulate ex vivo expansion of human cord blood hematopoietic stem cells as assayed by NOD/SCID transplantation. Blood 111, 3415–3423 (2008). [PubMed: 18202223]
61. Rocke DM & Durbin B A model for measurement error for gene expression arrays. J. Comput. Biol 8, 557–569 (2001). [PubMed: 11747612]
62. Dozmorov I & Centola M An associative analysis of gene expression array data. Bioinformatics 19, 204–211 (2003). [PubMed: 12538240]
63. Dozmorov I & Lefkovits I Internal standard-based analysis of microarray data. Part 1: analysis of differential gene expressions. Nucleic Acids Res. 37, 6323–6339 (2009). [PubMed: 19720734]
64. Kamburov A, Stelzl U, Lehrach H & Herwig R The ConsensusPathDB interaction database: 2013 update. Nucleic Acids Res. 41, D793–D800 (2013). [PubMed: 23143270]
65. Krämer A, Green J, Pollard J Jr. & Tugendreich S Causal analysis approaches in Ingenuity Pathway Analysis. Bioinformatics 30, 523–530 (2014). [PubMed: 24336805]

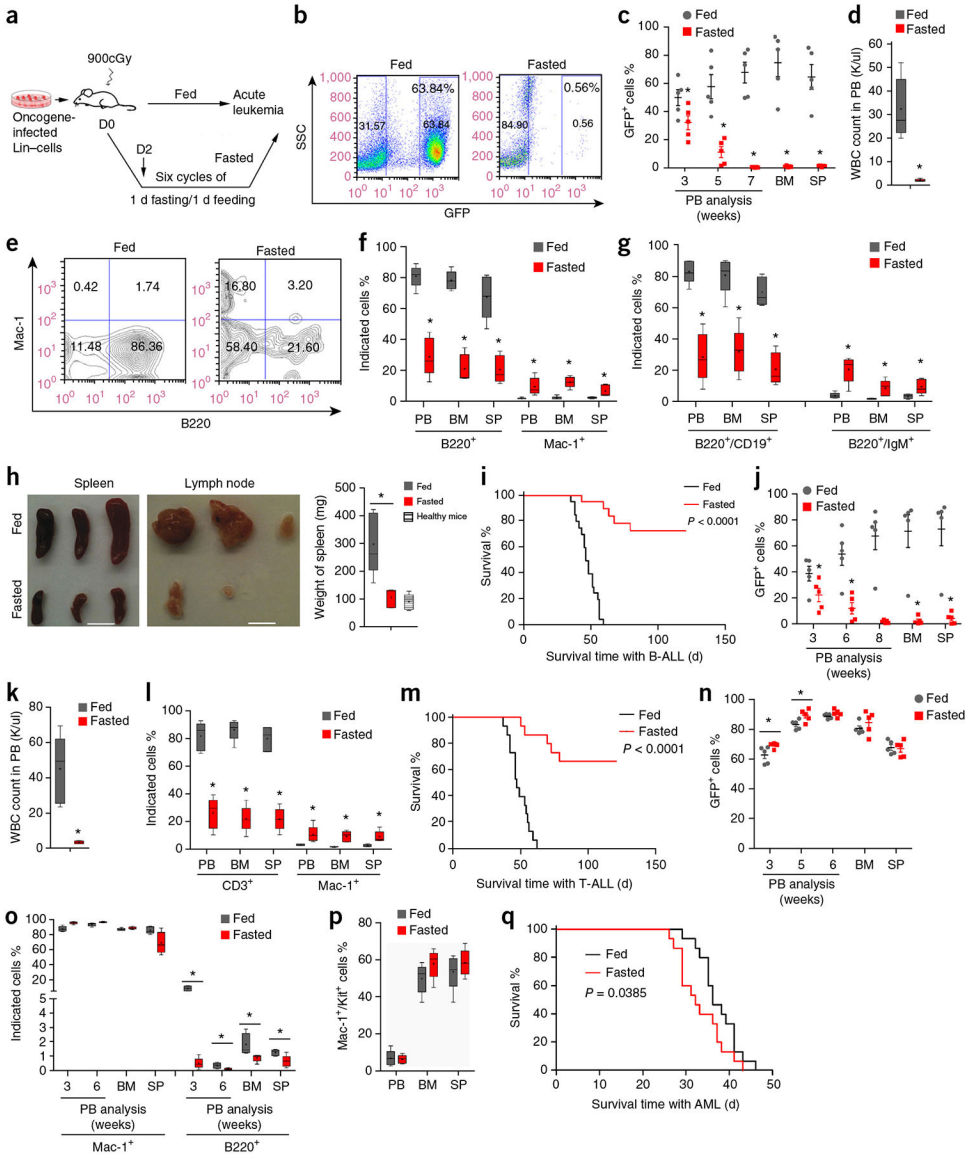

Figure 1.

Fasting selectively inhibits ALL development. (**a**) Leukemia induction and fasting scheme. Lin$^-$ cells were infected with N-Myc-IRES-GFP (B-ALL), Notch1-IRES-GFP (T-ALL), or MLL-AF9-IRES-YFP (AML) expressing retrovirus and transplanted into irradiated mice. Mice were fed normally or fasted with six cycles of 1-d fasting/1-d feeding at day 2 after transplantation. (**b–i**) N-Myc-infected Lin$^-$ cells were transplanted into lethally irradiated recipient mice to induce B-ALL. Mice were either placed on a standard diet or fasted (six cycles of 1-d fast/1-d fed), initiated at day 2 after transplantation. PB was analyzed at 3, 5 and 7 weeks after transplantation; BM and SP were collected at 7 weeks. (**b**) Representative flow cytometry plot of GFP$^+$ leukemic BM cells in fed and fasted mice. (**c**) Percentage of cells expressing GFP in PB at the indicated time points and in BM and SP (n = 5 mice per group). (**d**) WBC numbers in the PB at week 7 (n = 5 per group). (**e**) Representative flow cytometry plot of Mac-1 and B220 staining in GFP$^+$ BM cells in fed and fasted mice. (**f**)

Percentages of B220 and Mac-1 cells in GFP^+ cells from PB, BM and SP ($n = 5$ per group). (**g**) Analysis of B-ALL surface markers B220 (pan B cell marker), CD19 (B cell marker) and IgM (B cell maturation marker) in GFP^+ cells from PB, BM and SP ($n = 5$ per group). (**h**) Photographs of representative spleens and lymph nodes (left; scale bars, 1 cm) and quantitation of spleen weight (right) from fed and fasted mice with B-ALL and nonleukemic (healthy) mice ($n = 3$ per group). (**i**) Combined survival analysis of fed and fasted mice with N-Myc-driven B-ALL from four independent experiments ($n = 20$ per group). (**j–m**) Notch1-infected fetal liver Lin^- cells were transplanted into lethally irradiated recipient mice to induce T-ALL. Mice were placed on a standard diet or a six-cycle fasting regimen initiated at 2 d after transplantation. (**j**) Percentage of GFP^+ cells in PB at 3, 5 and 7 weeks and in BM and SP at 7 weeks post-transplantation ($n = 5$ per group). (**k**) WBC numbers in the PB at 7 weeks in fed and fasted mice ($n = 5$ per group). (**l**) Levels of surface markers CD3 and Mac-1 in GFP^+ cells of PB, BM and SP at 7 weeks. (m) Combined survival analysis of fed and fasted mice with Notch1-driven T-ALL from three independent experiments ($n = 15$ per group). (n–q) MLL-AF9-infected fetal liver Lin^- cells were transplanted into lethally irradiated recipient mice to induce AML. Mice were either placed on a standard diet or a six-cycle fasting regimen initiated at 2 d after transplantation. (**n**) Percentage of YFP^+ cells in PB at 3, 5 and 7 weeks and in BM and SP at 7 weeks ($n = 5$ per group). (**o**) Levels of surface markers Mac-1 and B220 in YFP^+ cells of PB, BM and SP at 6 weeks ($n = 5$ per group). (**p**) Levels of the AML progenitor marker c-Kit in PB, BM and SP at 6 weeks ($n = 5$ per group). (**q**) Combined survival analysis of fed and fasted mice with MLL-AF9-driven AML from three independent experiments ($n = 15$ per group). Representative data from three or four independent experiments are presented as dot plots (means ± s.e.m.) in c, j and n, or as box-and-whisker plots (median values (line), 25th–75th percentiles (box outline) and minimum and maximum values (whiskers)) in **d**, **f–h**, **k**, **l**, **o** and **p**. In **b** and **e**, numerals in outlined area indicate the percentage of cells in the gates or in each quantile. Statistical significance was calculated by Student's *t*-test, $*P < 0.05$. Statistical significance for survival in **i**, **m** and **q** was calculated by the log–rank test.

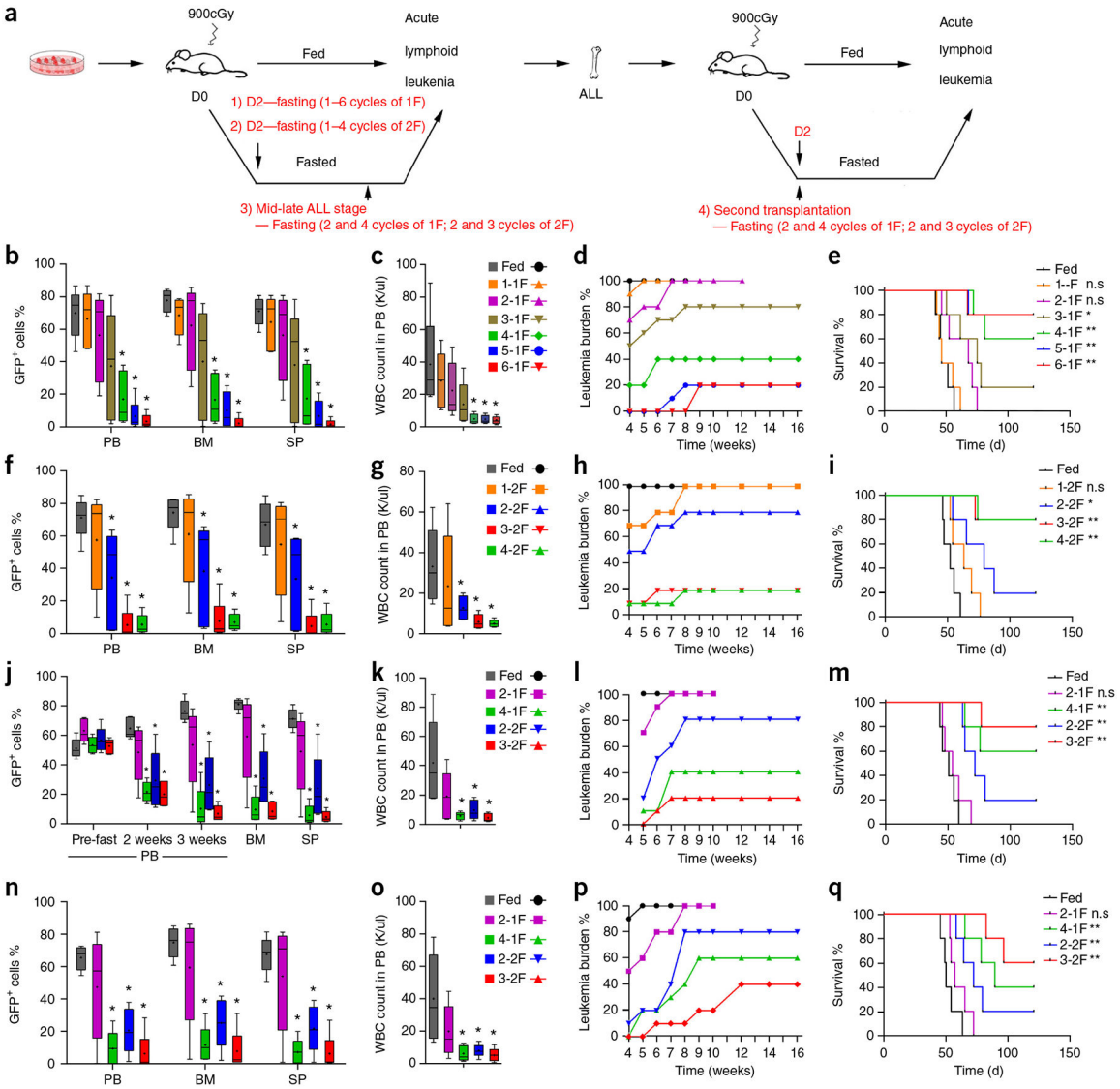

Figure 2.

Fasting inhibits B-ALL development in both early and late stages. (a) Leukemia induction and fasting regimens. Shown are regimens for fasting at an early stage (1 and 2) and at a mid-to-late stage (3) of primary B-ALL development, or in secondary B-ALL development (4). (**b–i**) N-Myc-infected Lin$^-$ cells were transplanted into lethally irradiated recipient mice to induce B-ALL. One to six cycles of 1-d fasting/1-d feeding (1F) (**b–e**) or one to four cycles of 2-d fasting/2-d feeding (2F) (**f–i**) were initiated at 2 d post-transplantation. (**b,f**) Percentage of GFP$^+$ cells in PB, BM and SP at 7 weeks post-transplantation (n = 5 per group). (**c,g**) WBC numbers in PB at 7 weeks post-transplantation (n = 5 per group). (**d,h**) Leukemia burden rates, defined as >20% of GFP$^+$ cells in PB with no decrease in the percentage of GFP$^+$ cells as compared to the prior week, at the indicated time points (n = 10 per group before and at week 7, and n = 5 per group after week 7). (**e,i**) Survival of mice with B-ALL (n = 5 per group). (**j,g**) N-Myc-infected Lin$^-$ cells were transplanted into lethally irradiated recipient mice, and two and four-cycles of 1F or two and three-cycles of

2F fasting were initiated when the percentage of GFP^+ cells in PB reached ~60% (at around 3–4 weeks). (**j**) Percentage of GFP^+ cells in PB before fasting was initiated and at 2 and 3 weeks after fasting, and in BM and SP at 3 weeks after fasting ($n = 5$ per group). (**k**) WBC numbers in PB 3 weeks after fasting ($n = 5$ per group). (**l**) Leukemia burden rates at the indicated time points ($n = 10$ per group before and at week 7, and $n = 5$ per group after week 7). (**m**) Survival analysis of B-ALL mice ($n = 5$ per group). (n–q) GFP^+ cells from the BM of primary N-Myc-induced B-ALL mice were transplanted into lethally irradiated recipient mice. Two and four-cycles of 1F or two and three-cycles of 2F fasting were initiated at 2 d after transplantation. (**n**) Percentage of GFP^+ cells in PB, BM, and SP at 8 weeks post-transplantation ($n = 5$ per group). (**o**) WBC numbers in PB at 8 weeks post-transplantation ($n = 5$ per group). (**p**) Leukemia burden rates mice at the indicated weeks ($n = 10$ per group before and at week 7, and $n = 5$ per group after week 7). (**q**) Survival of secondary B-ALL mice ($n = 5$ per group). Data in **b**, **c**, **f**, **g**, **j**, **k**, **n** and **o**, are presented as box-and-whisker plots (median values (line), 25th–75th percentiles (box outline) and minimum and maximum values (whiskers)). Statistical significance was calculated by Student's *t*-test, $*P < 0.05$. Statistical significance for survival analysis in **e**, **i**, **m** and **q** was calculated by the log–rank test, $*P < 0.05$, $**P < 0.01$.

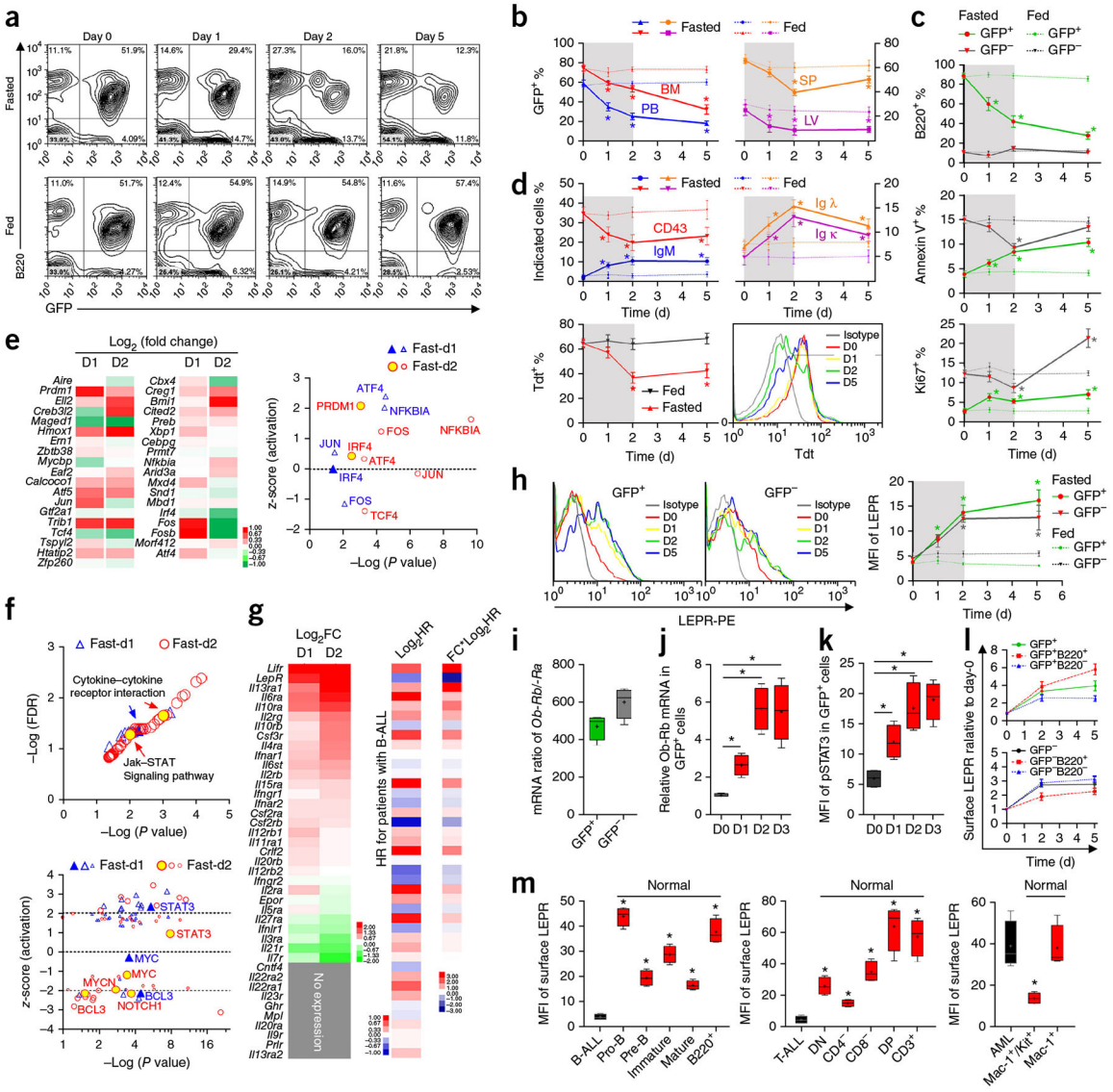

Figure 3.

Fasting upregulates LEPR expression and its downstream signaling. (**a**–**h**) N-Myc-infected Lin$^-$ cells were transplanted into lethally irradiated recipient mice, and a 48-h fast was initiated when the percentage of GFP$^+$ cells in PB reached ~60% (at around 3–4 weeks). Analyses were conducted before initiation of fasting and at days 1, 2 and 5 after initiation of fasting. (**a**) Representative flow cytometry plots showing GFP and B220 staining in PB of fasted and fed mice at the indicated time points. Numerals in the outlined area indicate the percentage of cells in each quantile. (**b**) The percentages of GFP$^+$ cells in PB, BM, SP and LV from fasted and fed mice at the indicated time points (n = 5 per group). (c) The percentages of B220$^+$, Annexin V$^+$ and Ki67$^+$ cells in the GFP$^+$ and GFP$^-$ compartments from BM of fasted and fed mice (n = 5 per group). (**d**) The percentages of CD43$^+$, IgM$^+$, Igκ$^+$, Igλ$^+$ and Tdt$^+$ cells in the GFP$^+$B220$^+$ B-ALL cell compartment from BM of fasted and fed mice (n = 5 per group). A representative flow cytometry plot of Tdt staining is also shown (lower right). (**e**,**f**) GFP$^+$B220$^+$ B-ALL cells from 1-d (D1) or 2-d (D2) fasted mice,

and control mice were sorted for RNA-seq analysis. (**e**) Fasting induced alterations of signature transcription factors of B cell terminal differentiation, shown for mRNA levels (fasted versus fed, left) and inferred activities (fasted versus fed, right). (**f**) Fasting-induced alterations in pathways (top) and transcription factor activities (fasted versus fed, bottom). (**g**) Relative mRNA expression (log_2-fold change, FC) of all 42 cytokine receptors in the KEGG pathway database in the sorted cells by qPCR (fasted versus fed, left), the log_2 values of their original hazard ratios (HRs) (middle) and their mRNA fold change normalized hazard ratios (log_2 HR multiplied by fold change) for survival of human pediatric patients with pre-B-ALL. Up- and downregulation of mRNA levels are indicated by red and green, respectively; HRs below and above 1 are indicated by blue and red, respectively. (**h**) Representative flow cytometry plots (left and middle) and quantitation (right) of LEPR staining (mean fluorescence intensity, MFI) in GFP^+ and GFP^- BM cell populations from fasted and fed mice at the indicated time points. ($n = 5$ per group). (**i**) Ratio of *Lepr* mRNA isoforms *Ob-Rb* to *Ob-Ra* in GFP^+ and GFP^- PB cells of fed B-ALL mice, by qPCR ($n = 4$ per group). (**j**) Fold change of *Ob-Rb* mRNA in BM GFP^+ cells of fasted mice at the indicat ed time points, by qPCR ($n = 5$ per group). (**k**) Quantitation of phospho-STAT3 staining in BM GFP^+ cells from fasted mice at the indicated time points ($n = 5$ per group). (**l**) Fold change of surface LEPR in the indicated populations of BM cells relative to pre-fast levels ($n = 5$ per group). (**m**) Comparison of surface LEPR expression on N-Myc B-ALL cells, Notch1 T-ALL cells and MLL-AF9 AML cells with normal BM B, T and myeloid cell subpopulations: pro-B ($B220^+IgM^-CD43^+$), Pre-B ($B220^+IgM^-CD43^-$), immature-B ($B220^+IgM^+IgD^-$), mature-B ($B220^+IgM^+IgD^+$) and total $B220^+$ cells (B cell subpopulations); DN ($CD3^+CD4^-CD8^-$), $CD3^+CD4^-$, $CD3^+CD8^-$, DP ($CD3^+CD4^+CD8^+$) and total $CD3^+$ cells (T cell subpopulations); and $Mac1^+cKit^+$ myeloid progenitors and total $Mac1^+$ cells (myeloid cell subpopulations) ($n = 5$ per group). Representative data from three independent experiments are presented as means ± s.e.m. in **b**–**d**, **h** and **l**, or as box-and-whisker plots (median values (line), 25th–75th percentiles (box outline) and minimum and maximum values (whiskers)) in **i**–**k** and **m**. In statistical significance was calculated by Student's *t*-test, $*P < 0.05$.

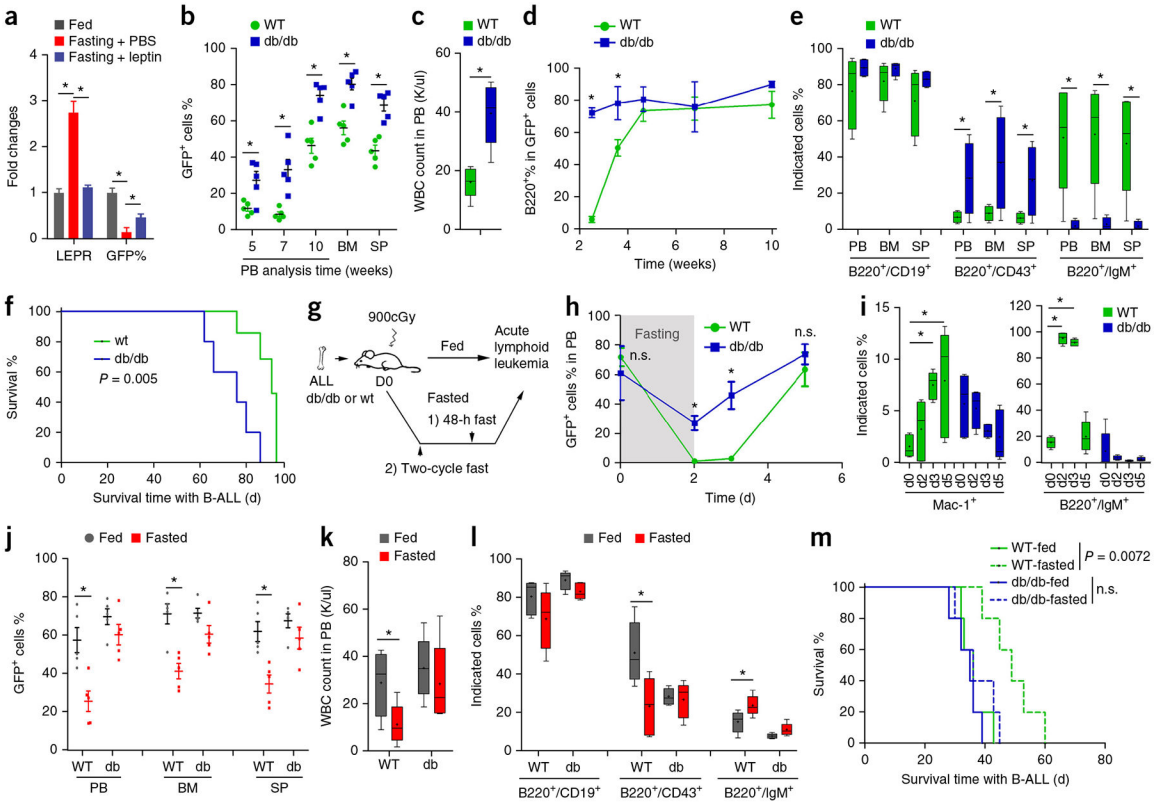

Figure 4.

Attenuated LEPR signaling is essential for ALL development, and fasting does not inhibit B-ALL development in the absence of LEPR. (**a**) B-ALL mice were fasted for 48 h with administration of leptin (5 μg/15 g body weight) or PBS when the percentage of GFP$^+$ cells in PB reached ~60%. The percentage of GFP$^+$ cells and surface LEPR expression on GFP$^+$B220$^+$ B-ALL cells were measured by flow cytometry and compared with pre-fast levels (n = 3 per group). (**b**–**f**) N-Myc-infected Lin$^-$ BM cells from wild-type (wt) or *Lepr*$^{db/db}$ mice were transplanted into lethally irradiated wild-type recipient mice. (**b**) Percentage of GFP$^+$ cells in PB at 5, 7, and 10 weeks post-transplantation and in BM and SP at 10 weeks (n = 5 per group). (**c**) WBC numbers at 10 weeks (n = 5 per group). (**d**) Percentage of B220$^+$ cells in the GFP$^+$ compartment in PB at the indicated time points (n = 5 per group). (**e**) Percentage of cells positive for the surface markers B220, CD19, CD43 and IgM in the GFP$^+$ compartment in PB, BM and SP at 10 weeks post-transplantation. (**f**) Survival analysis of wild-type (wt) and *Lepr*$^{db/db}$ mice with N-Myc-induced B-ALL (wt, n = 6; db/db, n = 5). (**g**) Schematic of leukemia initiation and the two fasting regimens. N-Myc-infected Lin- BM cells from wild-type (wt) or *Leprdb/db* mice were transplanted into lethally irradiated wild-type recipient mice. Approximately 104 GFP$^+$ B-ALL cells from these primary B-ALL mice were sorted and transplanted into lethally irradiated secondary recipient mice. The mice were fed normally or subjected to either of two fasting regimens: a 48-h fast was initiated when the percentage of GFP$^+$ cells in PB reached ~60%, or two cycles of 2-d fasting/2-d feeding were performed beginning at 2 d after transplantation. (**g**–**i**) 48-h fast regimen, as shown in **g**. (**h**) Percentage of GFP$^+$ cells in PB at the indicated time points after fasting was initiated (n = 5 per group). (**i**) Percentage of Mac-1$^+$/B220$^-$ myeloid cells and B220$^+$/IgM$^+$

differentiated cells in GFP^+ cells from PB at the indicated time points after fasting was initiated ($n = 5$ per group). (**j**–**m**) Two-cycle fast regimen, as shown in **g**. (**j**) Percentage of GFP^+ cells in PB, BM and SP at 5 weeks post-transplantation ($n = 5$ per group). (**k**) WBC numbers in PB at 5 weeks post-transplantation ($n = 5$ per group). (**l**) Surface marker expression, including B220, CD19, CD43 and IgM, on BM GFP^+ cells at 5 weeks post-transplantation ($n = 5$ per group). (**m**) Survival analysis ($n = 5$ per group). Representative data from three independent experiments are presented as means ± s.d. in **a**, **d** and **h**, or as dot plots (means ± s.e.m.) in **b** and **j**, or as box-and-whisker plots (median values (line), 25th–75th percentiles (box outline) and minimum and maximum values (whiskers)) in **c**, **e**, **i**, **k** and **l**. Statistical significance was calculated by Student's *t*-test, $*P < 0.05$. n.s., not significantly different. Statistical significance for survival analysis in **f** and **m** was calculated by the log–rank test.

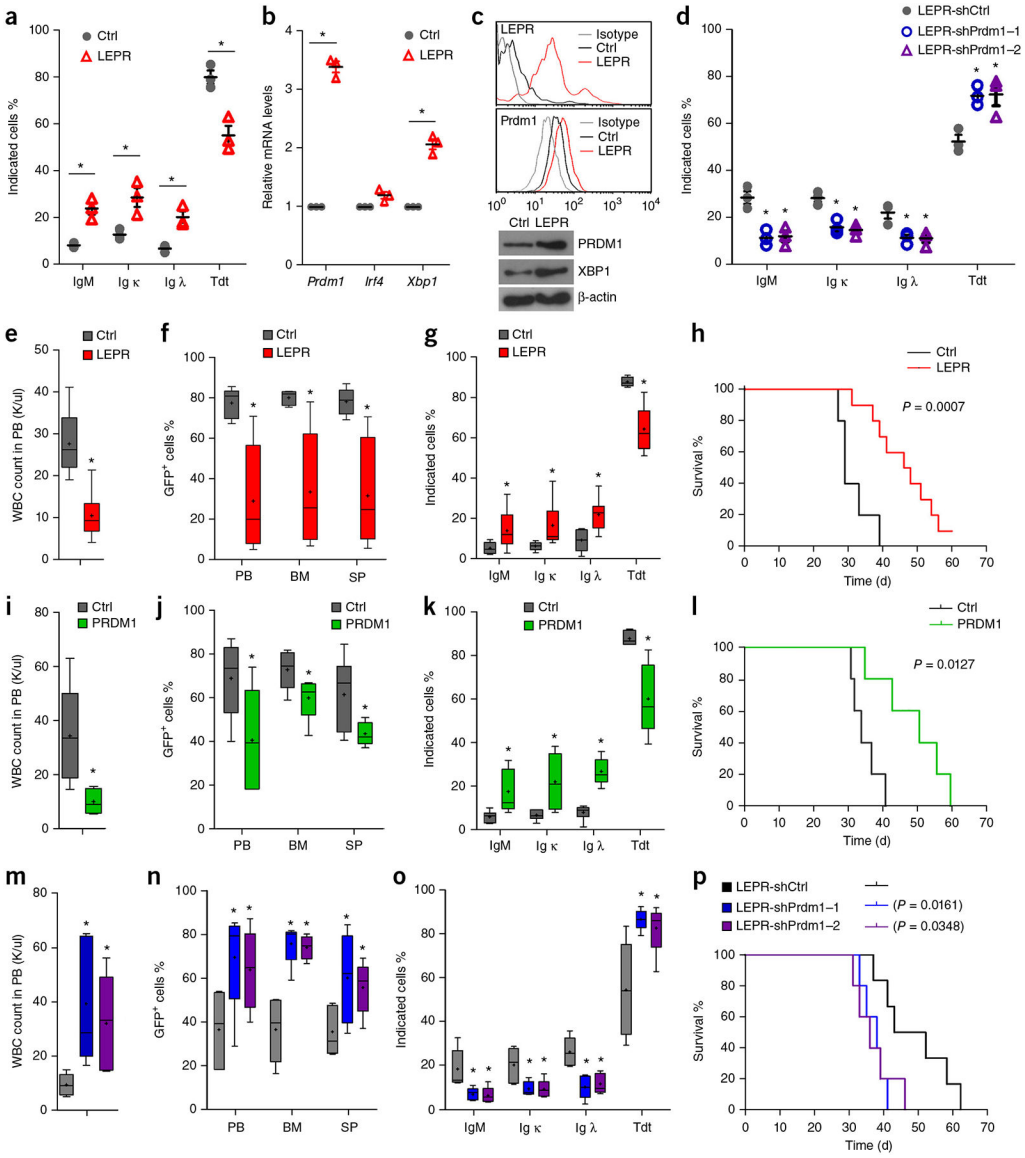

Figure 5.

LEPR inhibits B-ALL development by promoting leukemic cell differentiation through PRDM1. (**a**–**c**) Primary mouse B-ALL cells from BM were infected with LEPR- or DsRed control (Ctrl)-expressing retrovirus and cultured for 2 d. (**a**) Percentages of IgM$^+$, Igκ^+, Igλ^+ and Tdt$^+$ cells in the GFP$^+$ compartment, by flow cytometry ($n = 3$ per group). (**b**) Relative mRNA levels of *Prdm1*, *Irf4* and *Xbp1* in the GFP$^+$ compartment, by qPCR ($n = 3$ per group). (**c**) Representative flow cytometry plot showing LEPR staining (top) and PRDM1 intracellular staining (middle), and a representative western blot for PRDM1 and XBP1 (bottom) in the GFP$^+$ compartment. (**d**) BM cells from primary B-ALL mice were infected with LEPR-expressing retrovirus together with shCtrl- or shPRDM1-expressing lentivirus (with a DsRed reporter) and cultured for 2 d. The percentages of IgM$^+$, Igκ^+, Igλ^+ and Tdt$^+$ cells in *Lepr*$^+$DsRed$^+$GFP$^+$ B-ALL cells were measured by flow cytometry ($n = 3$ per group). (**e**–**h**) BM cells from primary B-ALL mice were infected with LEPR- or DsRed

(Ctrl) expressing retrovirus. GFP^+*Lepr*$^+$ or GFP^+DsRed^+ cells were sorted, and 1 × 104 double-positive cells per mouse were transplanted into lethally irradiated mice together with normal cell competitors. (**e**) WBC numbers in PB at week 4 ($n = 5$ per group). (**f**) The percentage of GFP cells in PB, BM and SP at week 4, by flow cytometry ($n = 5$ per group). (**g**) Expression of Tdt, surface IgM, Igκ and Igλ on BM GFP^+ cells at week 4, by flow cytometry ($n = 5$ per group). (**h**) Survival analysis (Ctrl group, $n = 5$; LEPR group, $n = 10$). (**i**–**l**) BM cells from mice with B-ALL were infected with PRDM1- or DsRed (Ctrl)-expressing retrovirus. GFP^+DsRed^+ cells were sorted, and 1 × 104 double-positive cells per mouse were transplanted into lethally irradiated mice together with normal cell competitors. (**i**) WBC numbers in PB at week 4 ($n = 5$ per group). (**j**) The percentage of GFP^+ cells in PB, BM and SP at week 4, by flow cytometry ($n = 5$ per group). (**k**) Expression of Tdt, surface IgM, Igκ and Igλ on BM GFP^+ cells at week 4, by flow cytometry ($n = 5$ per group). (l) Survival analysis ($n = 5$ per group). (**m**–**p**) GFP^+ BM cells from B-ALL mice were infected with LEPR-expressing retrovirus together with shCtrl- or shPRDM1-expressing lentivirus (with a DsRed reporter). $GFP^+LEPR^+DsRed^+$ cells were sorted, and 1 × 104 sorted cells were transplanted per mouse into lethally irradiated mice together with normal cell competitors. (**m**) WBC numbers in PB at week 4 ($n = 5$ per group). (**n**) The percentage of GFP^+ cells in PB, BM and SP at week 4, by flow cytometry ($n = 5$ per group). (**o**) Expression of Tdt, surface IgM, Igκ and Igλ on GFP^+ BM cells at week 4, by flow cytometry ($n = 5$). (**p**) Survival analysis (shCtrl, $n = 6$; shPRDM1, $n = 5$ per group). Colors in **m**–**o** as in **p**. Representative data from three independent experiments are presented as dot plots (means ± s.e.m.) in **a**, **b** and **d**, or as box-and-whisker plots (median values (line), 25th–75th percentiles (box outline) and minimum and maximum values (whiskers)) plots in **e**–**g**, **i**–**k**, and **m**–**o**. Statistical significance was calculated by Student's *t*-test, $*P < 0.05$. Statistical significance for survival analysis in **h**, **i** and **p** was calculated by the log–rank test.

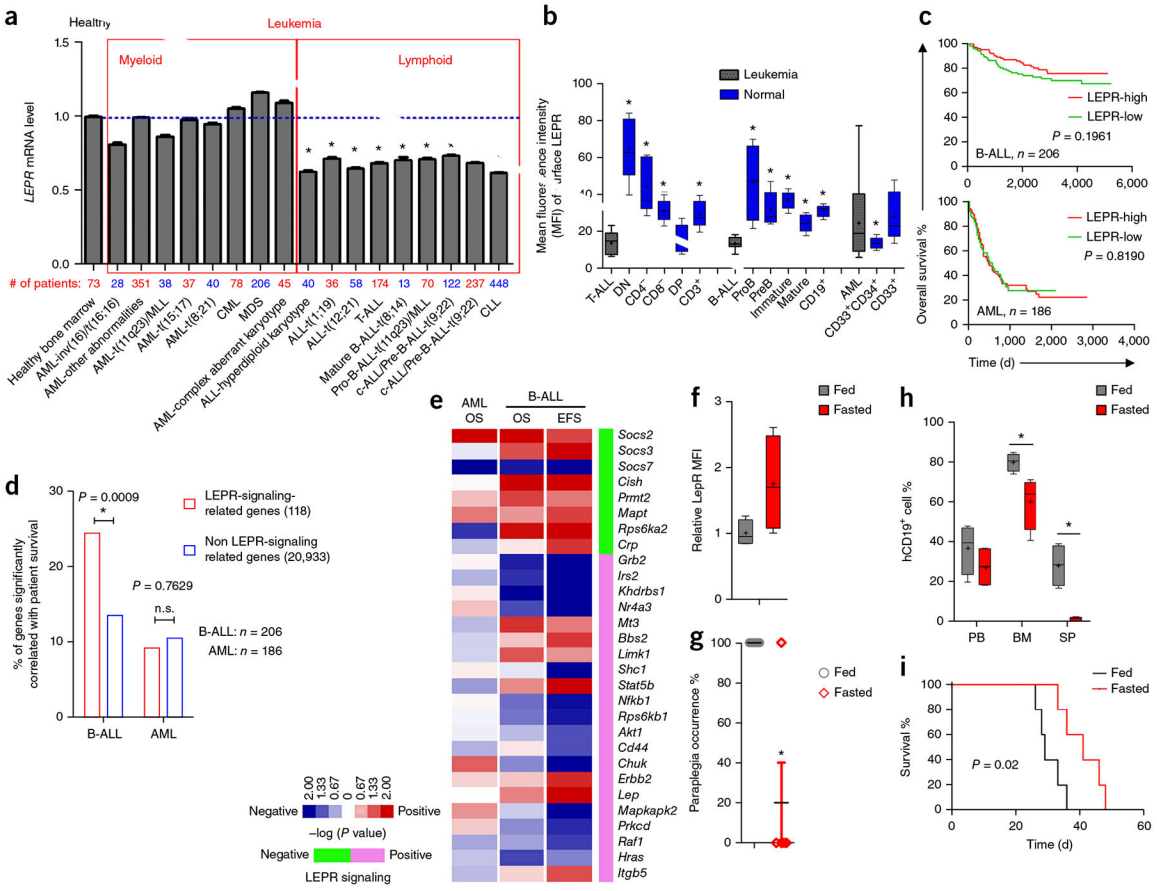

Figure 6.

Fasting and LEPR signaling inhibit human ALL development. (**a**) *LEPR* mRNA levels in the indicated types of human lymphoid leukemia and myeloid leukemia samples relative to healthy bone marrow samples (GEO data set GSE13159, $n = 2096$). (**b**) Flow cytometry analysis showing surface LEPR on human patient T-ALL ($CD3^+$, $n = 5$ patients), B-ALL ($CD19^+$, $n = 8$ patients) and AML ($CD33^+$, $n = 52$ patients) cells; on human cord blood-derived normal T cell subpopulations including DN ($CD3^+CD4^-CD8^-$), $CD3^+CD4^-$, $CD3^+CD8^-$, DP ($CD3^+CD4^+CD8^+$) and total $CD3^+$ T cells; normal B cell subpopulations including Pro-B ($CD19^+CD34^+CD38^+$), Pre-B ($CD19^+CD34^+CD40^+$); immature-B ($CD19^+CD40^+IgM^+$), mature-B ($CD19^+IgM^+IgD^+$) and total $CD19^+$ B cells; and myeloid subpopulations including $CD33^+CD34^+$ myeloid progenitors and $CD33^+$ myeloid cells (for all normal cell populations, $n = 5$ healthy donors per group). (**c**) Overall survival of pediatric patients with pre-B-ALL patients (COG P9906, $n = 206$) and patients with AML (TCGA, $n = 186$) relative to *LEPR* mRNA expression levels (above (high) or below (low) the 50th percentile). (**d**) Correlation analysis of the expression of LEPR-signaling-related genes (118) and nonrelated genes (20933) with overall survival (OS) and event-free survival (EFS) of patients with B-ALL, or with the overall survival of patients with AML. (**e**) Correlation analysis of the expression of 29 leptin/LEPR-signaling related genes with OS of patients with AML, or OS and EFS of patients with B-ALL. Positive and negative correlations with patient survival are indicated by red and blue, respectively; genes that are negatively or

positively associated with LEPR signaling are indicated in the bar on the far right as green or pink, respectively. (**f**) Expression of surface *LEPR* on human BM CD19$^+$ NALM-6 cells, by flow cytometry, in *scid* mice xenografted with 5 × 106 human B-ALL NALM-6 cells, which were fed or subjected to a 48-h fasting regimen initiated at day 10 after cell injection ($n = 5$ per group). (**g**–**i**) Xenografted mice as in **f** were fed or subjected to three cycles of 2-d fasting/2-d feeding initiated on day 2 after cell injection, and analyses were performed on day 25. (**g**) Paraplegia occurrence ($n = 5$ per group). (**h**) Percentage of human CD19$^+$ NALM-6 cells in PB, BM and SP, by flow cytometry ($n = 5$ per group). (**i**) Survival analysis ($n = 5$ per group). Data are presented as means ± s.e.m. in **a**, or as dot plot (means ± s.e.m.) in **g**, or as box-and-whisker plots (median values (line), 25th–75th percentiles (box outline) and minimum and maximum values (whiskers)) in **b**, **f** and **h**. Statistical significance was calculated by Student's *t*-test, $^*P < 0.05$. Statistical significance in **d** was calculated by the χ-squared test. Statistical significance for survival analysis in **c**, **e** and **i** was calculated by the log–rank test.